*Journal of Atmospheric Chemistry* 7 (1988), 107–135.



# Ultraviolet Absorption Cross-Sections of Chloro and Chlorofluoro-Methanes at Stratospheric Temperatures

P. C. SIMON, D. GILLOTAY, N. VANLAETHEM-MEUREE, and J. WISEMBERG
*Institut d'Aéronomie Spatiale de Belgique, 3, Avenue Circulaire, B1180 Brussels, Belgium*

(Received: 7 October 1987)

**Abstract.** Absorption cross-sections of nine halomethanes ($CCl_4$, $CHCl_3$, $CH_2Cl_2$, $CH_3Cl$, $CFCl_3$, $CF_2Cl_2$, $CF_3Cl$, $CHFCl_2$, and $CHF_2Cl$), measured between 174 and 250 nm for temperatures ranging from 225 to 295 K, are presented with uncertainties ranging from 2 to 4% and compared with previous determinations made for comparable temperature ranges.

The largest temperature effect which takes place near the absorption threshold, decreases the absorption cross-section up to 50% for highly chlorinated methanes, but is negligible for molecules highly stabilized by hydrogen and/or fluorine. Extrapolated values for temperatures of aeronomical interest are presented, as well as parametrical formulas which give absorption cross-section values for given wavelength and temperature ranges.

**Key words.** Chloromethanes, chlorofluoromethanes, ultraviolet absorption, photodissociation coefficients, temperature dependence.

## 1. Introduction

Odd chlorine (Cl, ClO, $ClONO_2$, HCl, HOCl, . . .), which plays a key role in the budget of ozone in the stratosphere, is produced essentially by decomposition of halocarbons released in the troposphere. Organic halocarbons carbons containing hydrogen atoms such as $CHCl_3$, $CH_2Cl_2$, $CH_3Cl$, $CHFCl_2$, $CHF_2Cl$, may react rapidly with radicals such as OH and may thus be largely destroyed in the troposphere (Singh *et al.*, 1979). Fully halogenated compounds, such as $CFCl_3$, $CF_2Cl_2$, . . . , are not subject to chemical destruction in the troposphere and, therefore, are transported in the stratosphere where they are destroyed by photodissociation (Molina and Rowland, 1974). Actually, only molecules with appreciable tropospheric residence times are subject to the diffusion up to stratospheric altitudes. When emission data are considered simultaneously, it appears that at least $CF_2Cl_2$, $CFCl_3$, $CCl_4$, $CH_3Cl$, and $CHFCl_2$ play a significant roles in the stratospheric chemistry (WMO, 1985; Wuebbles, 1983; Schmidt *et al.*, 1985).

Since a significant fraction of the ozone loss in the 30–50 km region is due to active chlorine resulting from the photodecomposition of these halocarbons, the absorption cross-section of these molecules has to be known with a high accuracy. Furthermore, their temperature-dependence has to be carefully measured because of the temperature condition prevailing at stratospheric altitude.

Preliminary measurements of the temperature-dependence of absorption cross-sections of chlorofluoromethanes, published by Vanlaethem-Meuree *et al.* (1978), have shown some nonnegligible disagreements in the temperature-dependence of cross-sections with existing data (Chou *et al.*, 1976, 1977, 1978; Robbins, 1976a,b,c; Robbins and Stolarski,

1976; Bass and Ledford 1976). Even at room temperature, discrepancies between some data are larger than the experimental uncertainties.

The purpose of this paper is to report new measurements of the ultraviolet absorption cross-sections of nine halomethanes, namely: $CH_3Cl$, $CH_2Cl_2$, $CHCl_3$, $CCl_4$, $CF_3Cl$, $CF_2Cl_2$, $CFCl_3$, $CHF_2Cl$, and $CHFCl_2$ performed between 174 and 250 nm, at four different temperatures over the 225–295 K temperature range. This new set of data allows a reliable extrapolation down to 210 K. Taking into account the temperature dependence of the absorption cross-section and the stratospheric temperature profile, photodissociation coefficients are calculated showing a significant departure in these coefficients relative to similar calculations made for 295 K. These data will be helpful to quantitatively estimate the lifetime of these halomethanes and to perform more accurately chlorine and ozone budget evaluations in the stratosphere.

## 2. Experimental

Absorption cross-sections have been determined in the 200 nm wavelength range as a function of temperature, using classical single beam equipment (deuterium light source, 1 m model 225 McPherson monochromator, absorption cell, with an EMR 542 P.09.18 solar blind photomultiplier as the detector). A complete description of this experimental devise has previously been given by Wisemberg and Vanlaethem (1978) and Gillotay and Simon (1988).

Two different kinds of absorption cells were used to obtain the UV absorption spectra of the studied gases:

(1) As the condensation conditions restrict the use of fairly high gas pressures at low temperatures, a long absorption optical path is required to gain access to low absorption cross-section determination.

Most of the measurements have been performed by means of a thermostatic stainless absorption cell with a 2 m optical path. It can be evacuated down to $10^{-7}$ torr by an ionic pump which prevents contamination.

Temperature regulation down to 210 K is achieved by the circulation of cooled methylcyclohexane through a double jacket and thermal equilibrium is usually obtained after 3–4 hours, with a maximum temperature gradient between both ends of the cell of 2 K at 220 K.

Gas pressure is measured by three capacitance MKS-Baratron manometers, directly coupled to the absorption cell which enables the measurement of pressures ranging from $10^{-3}$ to 1000 torr with a precision better than 0.1%. Its decrease is followed during the cooling process. The actual gas temperature is determined by considering both the conditions prevailing at the three points of measurement in the cell and the value deduced from the pressure decrease, according to the perfect gases law. Both determinations are in close agreement, better than 2 K. Therefore, the accuracy of the final temperature determination is within 2 K over the whole temperature range.

For technical reasons, three temperatures have been selected for absorption cross-section measurements, namely around 270, 255, and 225 K.

Table I. Error budget

| (a) $T = 295$ K | % | % |
|---|---|---|
| Optical path (200 cm $\pm$ 0.1 cm) | 0.05 | |
| Pressure (in the range $10^3$–$2 \times 10^{-3}$ torr) | 0.1 | |
| Impurities in the sample | 0.1 | |
| Temperature ($\pm$0.1 K at 300 K) | 0.03 | |
| Absorbance $\ln(I_0/I)$ for $\tau = 1$ | 2.0 | |
| Total r.m.s. error ($2\sigma$) | $\pm$2.00 | |
| (b) $T = 210$ K | | |
| Optical path (200 cm $\pm$ 0.1 cm) | 0.05 | |
| Pressure (in the range $10^3$–$2 \times 10^{-3}$ torr) | 0.1 | |
| Impurities in the sample | 0.1 | |
| Temperature ($\pm$2 K at 210 K) | 1 | |
| Cross-section dependence on temperature error | 1 | |
| Absorbance $\ln(I_0/I)$ for $\tau = 1$ | 2.0 | |
| $= 0.6$ (min. value considered) | | 3.3 |
| Total r.m.s. error ($2\sigma$) | $\pm$2.47 | $\pm$3.62 |

(2) Some of the experiments were performed at room temperature in a 13.5 cm optical path absorption cell in order to gain access to the fairly high absorption cross-sections.

The agreement of the two sets of results is always within the experimental uncertainties defined below (2% at room temperature) in the overlap wavelength range.

Determination of the absorption cross-sections is based upon at least 15 sequential recordings of continuously scanned spectra of the incident and absorbed fluxes measured for identical temperature conditions, using Beer-Lambert's law.

$$I(\lambda) = I_0(\lambda) \exp(-\sigma(\lambda) n d) \tag{1}$$

where: $I_0(\lambda)$ and $I(\lambda)$ are, respectively, the incident and transmitted fluxes for a given wavelength, $n$ is the number of molecules per volume unit, $d$ is the optical path, and $\sigma(\lambda)$ is the absorption cross-section at wavelength $\lambda$. The spectral resolution is of 0.15 nm with 100 $\mu$m slits.

In all cases, measurements were performed in a wide pressure range, for which the validity of Beer–Lambert's law was confirmed.

All samples were of analytical grade and were distilled under vacuum and thoroughly outgassed before use.

According to the error budget, presented in Table I, the accuracy on cross-section measurements is of the order of $\pm$2%, at the ambient temperature. At lower temperatures, the uncertainties increased from $\pm$3% to $\pm$4% for the absorption cross-sections values lower than $2 \times 10^{-21}$ cm$^2$ molec$^{-1}$. Moreover, the standard deviation calculated, at each wavelength on the observed cross-sections values (at least 15 values), are lower than 2% at

Tables II–X

(a) Absorption cross-sections at 2 nm intervals for selected temperatures (295, 270, 250, 230, and 210 K)

(b) Absorption cross-sections over the spectral intervals used in atmospheric modeling calculations for selected temperatures (295, 270, 250, 230, and 210 K)

Table IIa. $CH_3Cl$

| $\lambda$ (nm) | $\sigma(\lambda) \times 10^{21}$ (cm$^2$ molec.$^{-1}$) | | | | |
|---|---|---|---|---|---|
| | 295 K | 270 K | 250 K | 230 K | 210 K |
| 174 | 1110 | 1110 | 1110 | 1110 | 1110 |
| 176 | 938 | 938 | 938 | 938 | 938 |
| 178 | 766 | 766 | 766 | 766 | 766 |
| 180 | 607 | 607 | 607 | 607 | 607 |
| 182 | 467 | 467 | 467 | 467 | 467 |
| 184 | 350 | 350 | 350 | 350 | 350 |
| 186 | 255 | 255 | 255 | 255 | 255 |
| 188 | 182 | 182 | 182 | 182 | 182 |
| 190 | 127 | 127 | 127 | 127 | 127 |
| 192 | 87.2 | 87.2 | 87.2 | 87.2 | 87.2 |
| 194 | 58.8 | 58.8 | 58.8 | 58.8 | 58.8 |
| 196 | 40.1 | 40.1 | 40.1 | 40.1 | 40.1 |
| 198 | 26.6 | 26.6 | 26.1 | 25.8 | 24.3 |
| 200 | 17.6 | 17.3 | 16.9 | 16.3 | 15.1 |
| 202 | 11.3 | 10.7 | 10.3 | 9.70 | 9.30 |
| 204 | 7.50 | 6.91 | 6.60 | 6.11 | 5.73 |
| 206 | 4.83 | 4.50 | 4.05 | 3.75 | 3.45 |
| 208 | 3.18 | 2.85 | 2.57 | 2.35 | 2.12 |
| 210 | 2.06 | 1.82 | 1.64 | 1.45 | 1.30 |
| 212 | 1.32 | 1.12 | 1.00 | 0.90 | 0.80 |
| 214 | 0.86 | 0.72 | 0.63 | 0.55 | 0.47 |
| 216 | 0.55 | 0.44 | 0.38 | 0.33 | 0.27 |

Table IIb. $CH_3Cl$ (wavenumber intervals: 500 cm$^{-1}$)

| No. | $\sigma(\lambda) \times 10^{21}$ (cm$^2$ molec.$^{-1}$) | | | | | |
|---|---|---|---|---|---|---|
| | $\lambda$ (nm) | 295 K | 270 K | 250 K | 230 K | 210 K |
| 45 | 173.9–175.4 | 1057 | 1057 | 1057 | 1057 | 1057 |
| 46 | 175.4–177.0 | 923 | 923 | 923 | 923 | 923 |
| 47 | 177.0–178.6 | 787 | 787 | 787 | 787 | 787 |
| 48 | 178.6–180.2 | 656 | 656 | 656 | 656 | 656 |
| 49 | 180.2–181.8 | 536 | 536 | 536 | 536 | 536 |
| 50 | 181.8–183.5 | 429 | 429 | 429 | 429 | 429 |
| 51 | 183.5–185.2 | 333 | 333 | 333 | 333 | 333 |
| 52 | 185.2–186.9 | 254 | 254 | 254 | 254 | 254 |
| 53 | 186.9–188.7 | 188 | 188 | 188 | 188 | 188 |
| 54 | 188.7–190.5 | 139 | 139 | 139 | 139 | 139 |
| 55 | 190.5–192.3 | 97.8 | 97.8 | 97.8 | 97.8 | 97.8 |

Table IIb. (*Continued*)

| No. | $\sigma(\lambda) \times 10^{21}$ (cm$^2$ molec.$^{-1}$) | | | | |
|---|---|---|---|---|---|
| | $\lambda$ (nm) | 295 K | 270 K | 250 K | 230 K | 210 K |
| 56 | 192.3–194.2 | 69.3 | 69.3 | 69.3 | 69.3 | 69.3 |
| 57 | 194.2–196.1 | 47.7 | 47.6 | 47.3 | 46.8 | 45.8 |
| 58 | 196.1–198.0 | 32.5 | 32.2 | 31.7 | 31.2 | 30.2 |
| 59 | 198.0–200.0 | 21.6 | 21.1 | 20.6 | 19.9 | 19.2 |
| 60 | 200.0–202.0 | 14.2 | 13.7 | 13.2 | 12.6 | 12.0 |
| 61 | 202.0–204.1 | 9.27 | 8.81 | 8.36 | 7.90 | 7.44 |
| 62 | 204.1–206.2 | 5.91 | 5.50 | 5.14 | 4.77 | 4.43 |
| 63 | 206.2–208.3 | 3.76 | 3.42 | 3.13 | 2.86 | 2.62 |
| 64 | 208.3–210.5 | 2.33 | 2.06 | 1.86 | 1.67 | 1.50 |
| 65 | 210.5–212.8 | 1.44 | 1.24 | 1.09 | 0.973 | 0.853 |
| 66 | 212.8–215.0 | 0.874 | 0.726 | 0.634 | 0.555 | 0.474 |
| 67 | 215.0–217.4 | 0.525 | 0.424 | 0.367 | 0.320 | 0.264 |

Table IIIa. $CH_2Cl_2$

| $\lambda$ (nm) | $\sigma(\lambda) \times 10^{21}$ (cm$^2$ molec.$^{-1}$) | | | | |
|---|---|---|---|---|---|
| | 295 K | 270 K | 250 K | 230 K | 210 K |
| 176 | 1850 | 1850 | 1850 | 1850 | 1850 |
| 178 | 1807 | 1807 | 1807 | 1807 | 1807 |
| 180 | 1695 | 1695 | 1695 | 1695 | 1695 |
| 182 | 1509 | 1509 | 1509 | 1509 | 1509 |
| 184 | 1307 | 1307 | 1307 | 1307 | 1307 |
| 186 | 1040 | 1040 | 1040 | 1040 | 1040 |
| 188 | 799 | 799 | 799 | 799 | 799 |
| 190 | 575 | 575 | 575 | 575 | 575 |
| 192 | 417 | 417 | 417 | 409 | 400 |
| 194 | 288 | 288 | 281 | 271 | 263 |
| 196 | 197 | 193 | 186 | 178 | 171 |
| 198 | 136 | 130 | 124 | 118 | 112 |
| 200 | 92.0 | 86.5 | 82.5 | 76.2 | 72.2 |
| 202 | 62.0 | 56.8 | 52.7 | 49.0 | 45.6 |
| 204 | 42.2 | 38.1 | 34.8 | 31.7 | 29.0 |
| 206 | 28.8 | 25.4 | 22.8 | 20.6 | 18.5 |
| 208 | 19.5 | 16.8 | 14.8 | 13.1 | 11.8 |
| 210 | 12.8 | 11.0 | 9.70 | 8.50 | 7.36 |
| 212 | 8.35 | 7.10 | 6.10 | 5.25 | 4.63 |
| 214 | 5.40 | 4.60 | 3.93 | 3.36 | 2.87 |
| 216 | 3.55 | 2.97 | 2.53 | 2.15 | 1.84 |
| 218 | 2.34 | 1.93 | 1.61 | 1.34 | 1.12 |
| 220 | 1.52 | 1.23 | 1.03 | 0.860 | 0.720 |

Table IIIb. $CH_2Cl_2$ (wavenumber intervals: 500 $cm^{-1}$)

| No. | $\lambda$ (nm) | $\sigma(\lambda) \times 10^{21}$ ($cm^2$ molec.$^{-1}$) | | | | |
|---|---|---|---|---|---|---|
| | | 295 K | 270 K | 250 K | 230 K | 210 K |
| 46 | 175.4–177.0 | 1847 | 1847 | 1847 | 1847 | 1847 |
| 47 | 177.0–178.6 | 1812 | 1812 | 1812 | 1812 | 1812 |
| 48 | 178.6–180.2 | 1783 | 1783 | 1783 | 1783 | 1783 |
| 49 | 180.2–181.8 | 1652 | 1652 | 1652 | 1652 | 1652 |
| 50 | 181.8–183.5 | 1470 | 1470 | 1470 | 1470 | 1470 |
| 51 | 183.5–185.2 | 1252 | 1252 | 1252 | 1252 | 1252 |
| 52 | 185.2–186.9 | 1040 | 1040 | 1040 | 1040 | 1040 |
| 53 | 186.9–188.7 | 801 | 801 | 801 | 801 | 801 |
| 54 | 188.7–190.5 | 621 | 621 | 621 | 621 | 621 |
| 55 | 190.5–192.3 | 457 | 454 | 450 | 442 | 435 |
| 56 | 192.3–194.2 | 335 | 330 | 325 | 316 | 309 |
| 57 | 194.2–196.1 | 238 | 232 | 226 | 218 | 211 |
| 58 | 196.1–198.0 | 167 | 160 | 155 | 148 | 141 |
| 59 | 198.0–200.0 | 113 | 108 | 102 | 96.5 | 91.4 |
| 60 | 200.0–202.0 | 76.7 | 71.5 | 67.1 | 62.4 | 58.4 |
| 61 | 202.0–204.1 | 51.6 | 47.3 | 43.7 | 40.1 | 37.0 |
| 62 | 204.1–206.2 | 33.9 | 30.5 | 27.7 | 25.0 | 22.8 |
| 63 | 206.2–208.3 | 22.2 | 19.6 | 17.5 | 15.6 | 14.0 |
| 64 | 208.3–210.5 | 14.2 | 12.3 | 10.8 | 9.48 | 8.38 |
| 65 | 210.5–212.8 | 9.07 | 7.71 | 6.66 | 5.77 | 5.02 |
| 66 | 212.8–215.0 | 5.64 | 4.71 | 4.02 | 3.43 | 2.95 |
| 67 | 215.0–217.4 | 3.47 | 2.86 | 2.42 | 2.04 | 1.73 |
| 68 | 217.4–219.8 | 2.06 | 1.69 | 1.42 | 1.18 | 0.995 |

Table IVa. $CHCl_3$

| $\lambda$ (nm) | $\sigma(\lambda) \times 10^{21}$ ($cm^2$ molec.$^{-1}$) | | | | |
|---|---|---|---|---|---|
| | 295 K | 270 K | 250 K | 230 K | 210 K |
| 174 | 4750 | 4750 | 4750 | 4750 | 4750 |
| 176 | 4930 | 4930 | 4930 | 4930 | 4930 |
| 178 | 4650 | 4650 | 4650 | 4650 | 4650 |
| 180 | 3875 | 3875 | 3875 | 3875 | 3875 |
| 182 | 3216 | 3216 | 3216 | 3216 | 3216 |
| 184 | 2425 | 2425 | 2425 | 2425 | 2425 |
| 186 | 1750 | 1750 | 1750 | 1750 | 1750 |
| 188 | 1395 | 1395 | 1395 | 1395 | 1395 |
| 190 | 1122 | 1122 | 1122 | 1122 | 1122 |
| 192 | 878 | 878 | 878 | 878 | 878 |
| 194 | 741 | 741 | 730 | 715 | 696 |
| 196 | 618 | 609 | 593 | 578 | 556 |
| 198 | 509 | 494 | 476 | 458 | 438 |
| 200 | 411 | 390 | 374 | 355 | 339 |
| 202 | 332 | 317 | 302 | 277 | 259 |
| 204 | 265 | 247 | 228 | 213 | 198 |
| 206 | 204 | 183 | 170 | 158 | 143 |
| 208 | 151 | 134 | 122 | 110 | 100 |
| 210 | 108 | 95.0 | 84.8 | 76.0 | 67.5 |

Table IVa. (*Continued*)

| λ (nm) | $\sigma(\lambda) \times 10^{21}$ (cm$^2$ molec.$^{-1}$) | | | | |
|---|---|---|---|---|---|
| | 295 K | 270 K | 250 K | 230 K | 210 K |
| 212 | 77.5 | 66.8 | 58.8 | 51.8 | 45.5 |
| 214 | 53.8 | 45.5 | 39.5 | 34.3 | 29.7 |
| 216 | 36.5 | 30.3 | 26.4 | 22.9 | 19.3 |
| 218 | 24.8 | 20.2 | 17.3 | 14.7 | 12.6 |
| 220 | 16.7 | 13.6 | 11.4 | 9.68 | 8.15 |
| 222 | 11.3 | 9.05 | 7.50 | 6.25 | 5.20 |
| 224 | 7.50 | 5.95 | 4.94 | 4.10 | 3.40 |
| 226 | 5.00 | 3.95 | 3.25 | 2.67 | 2.19 |
| 228 | 3.38 | 2.65 | 2.18 | 1.77 | 1.45 |
| 230 | 2.28 | 1.79 | 1.43 | 1.14 | 0.900 |
| 232 | 1.52 | 1.11 | 0.896 | 0.711 | 0.566 |
| 234 | 1.02 | 0.725 | 0.581 | 0.456 | 0.361 |
| 236 | 0.680 | 0.472 | 0.378 | 0.294 | 0.231 |
| 238 | 0.460 | 0.308 | 0.247 | 0.190 | 0.149 |
| 240 | 0.310 | 0.202 | 0.162 | 0.124 | 0.096 |

Table IVb. $CHCl_3$ (wavenumber intervals: 500 cm$^{-1}$)

| No. | λ (nm) | $\sigma(\lambda) \times 10^{21}$ (cm$^2$ molec.$^{-1}$) | | | | |
|---|---|---|---|---|---|---|
| | | 295 K | 270 K | 250 K | 230 K | 210 K |
| 45 | 173.9–175.4 | 4850 | 4850 | 4850 | 4850 | 4850 |
| 46 | 175.4–177.0 | 4929 | 4929 | 4929 | 4929 | 4929 |
| 47 | 177.0–178.6 | 4680 | 4680 | 4680 | 4680 | 4680 |
| 48 | 178.6–180.2 | 4145 | 4145 | 4145 | 4145 | 4145 |
| 49 | 180.2–181.8 | 3500 | 3500 | 3500 | 3500 | 3500 |
| 50 | 181.8–183.5 | 2930 | 2930 | 2930 | 2930 | 2930 |
| 51 | 183.5–185.2 | 2340 | 2340 | 2340 | 2340 | 2340 |
| 52 | 185.2–186.9 | 1750 | 1750 | 1750 | 1750 | 1750 |
| 53 | 186.9–188.7 | 1470 | 1470 | 1470 | 1470 | 1470 |
| 54 | 188.7–190.5 | 1180 | 1180 | 1180 | 1180 | 1180 |
| 55 | 190.5–192.3 | 920 | 920 | 920 | 920 | 911 |
| 56 | 192.3–194.2 | 790 | 790 | 790 | 774 | 754 |
| 57 | 194.2–196.1 | 665 | 658 | 645 | 631 | 608 |
| 58 | 196.1–198.0 | 560 | 546 | 529 | 515 | 493 |
| 59 | 198.0–200.0 | 455 | 437 | 419 | 403 | 382 |
| 60 | 200.0–202.0 | 367 | 347 | 328 | 312 | 295 |
| 61 | 202.0–204.1 | 295 | 274 | 257 | 242 | 226 |
| 62 | 204.1–206.2 | 228 | 209 | 193 | 180 | 165 |
| 63 | 206.2–208.3 | 168 | 151 | 137 | 126 | 114 |
| 64 | 208.3–210.5 | 118 | 104 | 92.6 | 85.0 | 75.5 |
| 65 | 210.5–212.8 | 82.0 | 70.5 | 62.3 | 56.2 | 49.2 |
| 66 | 212.8–215.0 | 55.0 | 46.5 | 40.1 | 35.7 | 30.8 |
| 67 | 215.0–217.4 | 35.5 | 29.5 | 25.2 | 22.2 | 18.8 |
| 68 | 217.4–219.8 | 21.8 | 17.9 | 15.1 | 12.9 | 10.9 |
| 69 | 219.8–222.2 | 13.5 | 10.9 | 9.11 | 7.69 | 6.48 |
| 70 | 222.2–224.7 | 8.35 | 6.64 | 5.51 | 4.59 | 3.84 |
| 71 | 224.7–227.3 | 5.00 | 3.95 | 3.25 | 2.67 | 2.19 |
| 72 | 227.3–229.9 | 2.95 | 2.29 | 1.87 | 1.50 | 1.25 |
| 73 | 229.9–232.6 | 1.76 | 1.34 | 1.08 | 0.860 | 0.677 |

Table Va. $CCl_4$

| $\lambda$ (nm) | $\sigma(\lambda) \times 10^{21}$ (cm$^2$ molec.$^{-1}$) | | | | |
|---|---|---|---|---|---|
| | 295 K | 270 K | 250 K | 230 K | 210 K |
| 174 | 9900 | 9900 | 9900 | 9900 | 9900 |
| 176 | 10100 | 10100 | 10100 | 10100 | 10100 |
| 178 | 9750 | 9750 | 9750 | 9750 | 9750 |
| 180 | 7200 | 7200 | 7200 | 7200 | 7200 |
| 182 | 5900 | 5900 | 5900 | 5900 | 5900 |
| 184 | 4400 | 4400 | 4400 | 4400 | 4400 |
| 186 | 3100 | 3100 | 3100 | 3100 | 3100 |
| 188 | 1980 | 1980 | 1980 | 1980 | 1980 |
| 190 | 1469 | 1469 | 1469 | 1469 | 1469 |
| 192 | 992 | 992 | 992 | 992 | 992 |
| 194 | 767 | 767 | 767 | 767 | 767 |
| 196 | 695 | 695 | 695 | 695 | 695 |
| 198 | 680 | 680 | 680 | 680 | 680 |
| 200 | 660 | 660 | 660 | 660 | 660 |
| 202 | 638 | 638 | 638 | 638 | 638 |
| 204 | 610 | 610 | 610 | 610 | 601 |
| 206 | 570 | 570 | 570 | 561 | 544 |
| 208 | 525 | 525 | 514 | 504 | 483 |
| 210 | 469 | 459 | 446 | 434 | 415 |
| 212 | 410 | 392 | 380 | 367 | 348 |
| 214 | 345 | 327 | 315 | 295 | 279 |
| 216 | 278 | 259 | 244 | 230 | 217 |
| 218 | 221 | 201 | 189 | 172 | 163 |
| 220 | 175 | 158 | 146 | 135 | 125 |
| 222 | 136 | 120 | 109 | 98.0 | 90.0 |
| 224 | 102 | 88.0 | 79.5 | 71.4 | 64.0 |
| 226 | 76.0 | 64.5 | 57.8 | 50.5 | 44.5 |
| 228 | 56.5 | 47.0 | 41.7 | 36.2 | 31.6 |
| 230 | 42.8 | 34.9 | 30.4 | 25.7 | 22.7 |
| 232 | 30.4 | 24.8 | 21.1 | 17.9 | 15.2 |
| 234 | 22.0 | 17.7 | 14.8 | 12.5 | 10.5 |
| 236 | 16.0 | 12.7 | 10.5 | 8.72 | 7.23 |
| 238 | 11.6 | 9.06 | 7.43 | 6.10 | 5.00 |
| 240 | 8.30 | 6.40 | 5.19 | 4.22 | 3.42 |
| 242 | 5.90 | 4.49 | 3.62 | 2.91 | 2.34 |
| 244 | 4.13 | 3.11 | 2.48 | 1.98 | 1.58 |
| 246 | 2.90 | 2.17 | 1.72 | 1.36 | 1.08 |
| 248 | 2.10 | 1.56 | 1.23 | 0.968 | 0.762 |
| 250 | 1.48 | 1.09 | 0.858 | 0.673 | 0.528 |

Table Vb. $CCl_4$ (wavenumber intervals: 550 $cm^{-1}$)

| No. | $\lambda$ (nm) | $\sigma(\lambda) \times 10^{21}$ ($cm^2$ molec.$^{-1}$) | | | | |
|---|---|---|---|---|---|---|
| | | 295 K | 270 K | 250 K | 230 K | 210 K |
| 45 | 173.9–175.4 | 10000 | 10000 | 10000 | 10000 | 10000 |
| 46 | 175.4–177.0 | 10000 | 10000 | 10000 | 10000 | 10000 |
| 47 | 177.0–178.6 | 9800 | 9800 | 9800 | 9800 | 9800 |
| 48 | 178.6–180.2 | 8150 | 8150 | 8150 | 8150 | 8150 |
| 49 | 180.2–181.8 | 6550 | 6550 | 6550 | 6550 | 6550 |
| 50 | 181.8–183.5 | 5350 | 5350 | 5350 | 5350 | 5350 |
| 51 | 183.5–185.2 | 4200 | 4200 | 4200 | 4200 | 4200 |
| 52 | 185.2–186.9 | 3100 | 3100 | 3100 | 3100 | 3100 |
| 53 | 186.9–188.7 | 1999 | 1999 | 1999 | 1999 | 1999 |
| 54 | 188.7–190.5 | 1510 | 1510 | 1510 | 1510 | 1510 |
| 55 | 190.5–192.3 | 1076 | 1076 | 1076 | 1076 | 1076 |
| 56 | 192.3–194.2 | 868 | 868 | 868 | 868 | 868 |
| 57 | 194.2–196.1 | 749 | 749 | 749 | 749 | 749 |
| 58 | 196.1–198.0 | 687 | 687 | 687 | 687 | 687 |
| 59 | 198.0–200.0 | 670 | 670 | 670 | 670 | 670 |
| 60 | 200.0–202.0 | 649 | 649 | 649 | 649 | 649 |
| 61 | 202.0–204.1 | 619 | 619 | 619 | 619 | 619 |
| 62 | 204.1–206.2 | 598 | 598 | 598 | 594 | 577 |
| 63 | 206.2–208.3 | 548 | 544 | 537 | 529 | 513 |
| 64 | 208.3–210.5 | 483 | 472 | 463 | 451 | 435 |
| 65 | 210.5–212.8 | 413 | 397 | 386 | 371 | 355 |
| 66 | 212.8–215.0 | 339 | 321 | 308 | 292 | 277 |
| 67 | 215.0–217.4 | 270 | 251 | 238 | 222 | 209 |
| 68 | 217.4–219.8 | 207 | 188 | 176 | 162 | 151 |
| 69 | 219.8–222.2 | 155 | 138 | 127 | 115 | 105 |
| 70 | 222.2–224.7 | 113 | 98.1 | 88.9 | 79.4 | 71.7 |
| 71 | 224.7–227.3 | 77.9 | 66.4 | 59.1 | 51.9 | 46.1 |
| 72 | 227.3–229.9 | 52.7 | 44.0 | 38.4 | 33.2 | 29.0 |
| 73 | 229.9–232.6 | 33.4 | 27.2 | 23.4 | 19.8 | 17.0 |
| 74 | 232.6–235.3 | 22.6 | 18.1 | 15.3 | 12.8 | 10.8 |
| 75 | 235.3–238.1 | 14.2 | 11.1 | 9.23 | 7.61 | 6.31 |
| 76 | 238.1–241.0 | 8.83 | 6.81 | 5.56 | 4.52 | 3.69 |
| 77 | 241.0–243.9 | 5.30 | 4.02 | 3.23 | 2.59 | 2.08 |
| 78 | 243.9–246.9 | 3.24 | 2.43 | 1.93 | 1.53 | 1.21 |
| 79 | 246.9–250.0 | 1.93 | 1.43 | 1.13 | 0.886 | 0.696 |

the ambient temperature. At the lowest temperature and for the lowest values of the absorption cross-section, the standard deviation is in the order of 3.5%, after the least-squares fit on the four studied temperatures.

## 3. Results

The numerical values of absorption cross-sections for selected wavelengths between 174 and 250 nm and wavenumber intervals of 500 $cm^{-1}$ currently used for aeronomy modelling (Brasseur and Simon, 1981) are given, respectively, in Tables IIa–Xa and IIb–Xb. The absorption spectra are also presented in Figures 1–6.

Table VIa. $CF_3Cl$

| $\lambda$ (nm) | $\sigma(\lambda) \times 10^{21}$ (cm$^2$ molec.$^{-1}$) |
|---|---|
| | 295 K |
| 172 | 11.0 |
| 174 | 9.70 |
| 176 | 8.25 |
| 178 | 6.81 |
| 180 | 5.42 |
| 182 | 4.25 |
| 184 | 3.26 |
| 186 | 2.44 |
| 188 | 1.75 |
| 190 | 1.28 |
| 192 | 0.900 |
| 194 | 0.610 |
| 196 | 0.410 |
| 198 | 0.280 |
| 200 | 0.190 |

Table VIb. $CF_3Cl$ (wavenumber intervals: 500 cm$^{-1}$

| No. | $\lambda$ (nm) | $\sigma(\lambda) \times 10^{21}$ (cm$^2$ molec.$^{-1}$) |
|---|---|---|
| | | 295 K |
| 43 | 169.5–172.4 | 11.7 |
| 44 | 172.4–173.9 | 10.3 |
| 45 | 173.9–175.4 | 9.25 |
| 46 | 175.4–177.0 | 8.10 |
| 47 | 177.0–178.6 | 6.95 |
| 48 | 178.6–180.2 | 5.80 |
| 49 | 180.2–181.8 | 4.80 |
| 50 | 181.8–183.5 | 3.90 |
| 51 | 183.5–185.2 | 3.10 |
| 52 | 185.2–186.9 | 2.44 |
| 53 | 186.9–188.7 | 1.80 |
| 54 | 188.7–190.5 | 1.36 |
| 55 | 190.5–192.3 | 0.990 |
| 56 | 192.3–194.2 | 0.700 |
| 57 | 194.2–196.1 | 0.480 |
| 58 | 196.1–198.0 | 0.320 |
| 59 | 198.0–200.0 | 0.220 |
| 60 | 200.0–202.0 | 0.150 |

Table VIIa. $CF_2Cl_2$

| $\lambda$ (nm) | $\sigma(\lambda) \times 10^{21}$ (cm$^2$ molec.$^{-1}$) | | | | |
|---|---|---|---|---|---|
| | 295 K | 270 K | 250 K | 230 K | 210 K |
| 174 | 1620 | 1620 | 1620 | 1620 | 1620 |
| 176 | 1810 | 1810 | 1810 | 1810 | 1810 |
| 178 | 1870 | 1870 | 1870 | 1870 | 1870 |
| 180 | 1790 | 1790 | 1790 | 1790 | 1790 |
| 182 | 1600 | 1600 | 1600 | 1600 | 1600 |
| 184 | 1340 | 1340 | 1340 | 1340 | 1340 |
| 186 | 1070 | 1070 | 1070 | 1070 | 1070 |
| 188 | 828 | 828 | 815 | 807 | 793 |
| 190 | 632 | 600 | 576 | 552 | 529 |
| 192 | 455 | 419 | 397 | 377 | 358 |
| 194 | 315 | 286 | 265 | 246 | 228 |
| 196 | 211 | 188 | 172 | 157 | 144 |
| 198 | 139 | 121 | 109 | 98.1 | 88.2 |
| 200 | 88.9 | 75.5 | 66.3 | 58.2 | 51.1 |
| 202 | 55.1 | 45.9 | 39.7 | 34.3 | 29.7 |
| 204 | 34.4 | 27.7 | 23.2 | 20.0 | 16.9 |
| 206 | 20.9 | 16.8 | 14.1 | 11.8 | 9.89 |
| 208 | 12.7 | 9.94 | 8.19 | 6.75 | 5.57 |
| 210 | 7.59 | 5.90 | 4.84 | 3.96 | 3.24 |
| 212 | 4.54 | 3.47 | 2.80 | 2.26 | 1.83 |
| 214 | 2.71 | 2.05 | 1.65 | 1.32 | 1.06 |
| 216 | 1.58 | 1.17 | 0.926 | 0.731 | 0.577 |
| 218 | 1.00 | 0.720 | 0.550 | 0.420 | 0.330 |
| 220 | 0.600 | 0.420 | 0.320 | 0.240 | 0.180 |
| 222 | 0.360 | 0.252 | 0.189 | 0.140 | 0.105 |
| 224 | 0.220 | 0.152 | 0.112 | 0.081 | 0.060 |
| 226 | 0.130 | 0.092 | 0.067 | 0.047 | 0.034 |

Table VIIb. $CF_2Cl_2$ (wavenumber intervals: 500 $cm^{-1}$)

| No. | $\lambda$ (nm) | $\sigma(\lambda) \times 10^{21}$ ($cm^2$ molec.$^{-1}$) | | | | |
|---|---|---|---|---|---|---|
| | | 295 K | 270 K | 250 K | 230 K | 210 K |
| 45 | 173.9–175.4 | 1700 | 1700 | 1700 | 1700 | 1700 |
| 46 | 175.4–177.0 | 1822 | 1822 | 1822 | 1822 | 1822 |
| 47 | 177.0–178.6 | 1860 | 1860 | 1860 | 1860 | 1860 |
| 48 | 178.6–180.2 | 1817 | 1817 | 1817 | 1817 | 1817 |
| 49 | 180.2–181.8 | 1700 | 1700 | 1700 | 1700 | 1700 |
| 50 | 181.8–183.5 | 1528 | 1528 | 1528 | 1528 | 1528 |
| 51 | 183.5–185.2 | 1310 | 1310 | 1310 | 1310 | 1310 |
| 52 | 185.2–186.9 | 1070 | 1070 | 1070 | 1070 | 1070 |
| 53 | 186.9–188.7 | 847 | 847 | 827 | 816 | 803 |
| 54 | 188.7–190.5 | 683 | 642 | 621 | 600 | 580 |
| 55 | 190.5–192.3 | 502 | 470 | 446 | 424 | 403 |
| 56 | 192.3–194.2 | 365 | 335 | 313 | 293 | 274 |
| 57 | 194.2–196.1 | 253 | 227 | 209 | 193 | 177 |
| 58 | 196.1–198.0 | 171 | 150 | 136 | 123 | 112 |
| 59 | 198.0–200.0 | 111 | 95.2 | 84.6 | 75.4 | 67.1 |
| 60 | 200.0–202.0 | 70.2 | 59.1 | 51.6 | 45.2 | 39.6 |
| 61 | 202.0–204.1 | 43.6 | 36.0 | 31.0 | 26.7 | 23.0 |
| 62 | 104.1–206.2 | 26.1 | 21.1 | 17.9 | 15.2 | 12.8 |
| 63 | 206.1–208.3 | 15.5 | 12.3 | 10.2 | 8.53 | 7.11 |
| 64 | 208.3–210.5 | 8.84 | 6.88 | 5.64 | 4.63 | 3.81 |
| 65 | 210.5–212.8 | 5.03 | 3.85 | 3.10 | 2.51 | 2.03 |
| 66 | 212.8–215.0 | 2.79 | 2.09 | 1.66 | 1.32 | 1.05 |
| 67 | 215.0–217.4 | 1.55 | 1.14 | 0.890 | 0.694 | 0.545 |
| 68 | 217.4–219.8 | 0.846 | 0.606 | 0.467 | 0.357 | 0.275 |
| 69 | 219.8–222.2 | 0.467 | 0.326 | 0.247 | 0.184 | 0.139 |
| 70 | 222.2–224.7 | 0.262 | 0.177 | 0.134 | 0.0954 | 0.0704 |
| 71 | 224.7–227.3 | 0.143 | 0.0927 | 0.0672 | 0.0471 | 0.0337 |

### 3.1. AMBIENT TEMPERATURE (295 K)

Cross-section measurements have been extended to lower values ($< 2 \times 10^{-21}$ $cm^2$ molec.$^{-1}$) than those currently available in the literature.

Chloro- and chlorofluoromethanes display continuous absorption in the 174–250 nm region, with absorption cross sections ranging from $10^{-17}$ to $10^{-22}$ $cm^2$ molec.$^{-1}$.

The progressive substitution of H atoms of the basic methane by Cl atoms leads to increased absorption and to an extended absorption region towards higher wavelengths, while, to the contrary, the presence of F atoms tends to stabilize the molecule whose absorption spectrum is depressed and shifted towards lower wavelengths.

The results presented in Table II–X and Figures 1–3 are, within the quoted accuracy, in close agreement with those generally used in modelling calculations (Codata panel, 1982; DeMore *et al.*, 1985) and confirm the previous published values for $CH_3Cl$ (Robbins, 1976,a,b), $CHCl_3$ (Robbins, 1976c), $CCl_4$ (Rowland and Molina, 1975; Robbins, 1976c), $CF_2Cl_2$ and $CFCl_3$ (Rowland and Molina, 1975; Robbins, 1976c; Robbins and Stolarski, 1976; Bass and Ledford, 1976; Chou *et al.*, 1977), and for $CHF_2Cl$ and $CHFCl_2$ (Robbins, 1976c; Robbins and Stolarski, 1976; Chou *et al.*, 1976) within the experimental errors.

Table VIIIa. $CFCl_3$

| $\lambda$ (nm) | $\sigma(\lambda) \times 10^{21}$ (cm$^2$ molec.$^{-1}$) | | | | |
|---|---|---|---|---|---|
| | 295 K | 270 K | 250 K | 230 K | 210 K |
| 174 | 3130 | 3130 | 3130 | 3130 | 3130 |
| 176 | 3240 | 3240 | 3240 | 3240 | 3240 |
| 178 | 3235 | 3235 | 3235 | 3235 | 3235 |
| 180 | 3140 | 3140 | 3140 | 3140 | 3140 |
| 182 | 2960 | 2960 | 2960 | 2960 | 2960 |
| 184 | 2720 | 2720 | 2720 | 2720 | 2720 |
| 186 | 2430 | 2385 | 2360 | 2335 | 2300 |
| 188 | 2130 | 2090 | 2070 | 2045 | 2020 |
| 190 | 1790 | 1760 | 1745 | 1725 | 1705 |
| 192 | 1540 | 1495 | 1465 | 1440 | 1412 |
| 194 | 1243 | 1218 | 1198 | 1174 | 1151 |
| 196 | 991 | 959 | 945 | 925 | 905 |
| 198 | 780 | 762 | 747 | 733 | 718 |
| 200 | 645 | 622 | 600 | 579 | 558 |
| 202 | 500 | 476 | 454 | 441 | 420 |
| 204 | 374 | 348 | 330 | 316 | 300 |
| 206 | 280 | 256 | 241 | 225 | 216 |
| 208 | 197 | 182 | 170 | 159 | 149 |
| 210 | 148 | 133 | 120 | 110 | 99.4 |
| 212 | 105 | 91.8 | 82.6 | 76.7 | 66.3 |
| 214 | 75.6 | 64.1 | 56.2 | 49.2 | 43.1 |
| 216 | 53.8 | 44.3 | 37.9 | 32.4 | 27.8 |
| 218 | 37.9 | 30.3 | 25.3 | 21.2 | 17.7 |
| 220 | 26.4 | 20.5 | 16.8 | 13.8 | 11.3 |
| 222 | 18.2 | 13.8 | 11.1 | 8.90 | 7.14 |
| 224 | 12.4 | 9.25 | 7.30 | 5.76 | 4.54 |
| 226 | 8.42 | 6.16 | 4.79 | 3.73 | 2.91 |
| 228 | 5.65 | 4.08 | 3.15 | 2.43 | 1.88 |
| 230 | 3.75 | 2.70 | 2.08 | 1.60 | 1.23 |

Disagreements of between 20 to 30% at some wavelengths are clearly seen from Figure 2, for $CF_2Cl_2$ between 204 and 210 nm and from Figure 4 for $CHF_2Cl$ between 198 and 204 nm.

In the case of methylene chloride ($CH_2Cl_2$), if one expects the data of Gordus and Bernstein (1954) limited to a narrow wavelength range (205–220 nm), the only available data are the values published by Hubrich and Stuhl (1980) which are, on average, 10% higher than those reported here.

Values obtained in this work for $CF_3Cl$ are significantly lower in the region of weak absorption (up to 30% depending of the wavelength) than the ones obtained by Chou *et al.* (1978) (not plotted on the figure) with a 10 cm absorption cell.

It should be pointed out that the use of a 2 m absorption cell allows a more accurate determination, especially in the ranges corresponding to low absorption.

With the assumption, in the first approximation, of an exponential decrease of absorption cross-sections with the wavelength in this low absorption region, the results presented here substantiate the hypothesis according to which tropospheric photodissociation is

Table VIIIb. $CFCl_3$ (wavenumber intervals: 500 $cm^{-1}$)

| No. | λ (nm) | $\sigma(\lambda) \times 10^{21}$ ($cm^2$ $molec.^{-1}$) | | | | |
|---|---|---|---|---|---|---|
| | | 295 K | 270 K | 250 K | 230 K | 210 K |
| 45 | 173.9–175.4 | 3180 | 3180 | 3180 | 3180 | 3180 |
| 46 | 175.4–177.0 | 3240 | 3240 | 3240 | 3240 | 3240 |
| 47 | 177.0–178.6 | 3238 | 3238 | 3238 | 3238 | 3238 |
| 48 | 178.6–180.2 | 3160 | 3160 | 3160 | 3160 | 3160 |
| 49 | 180.2–181.8 | 3050 | 3050 | 3050 | 3050 | 3050 |
| 50 | 181.8–183.5 | 2880 | 2880 | 2880 | 2880 | 2880 |
| 51 | 183.5–185-2 | 2670 | 2670 | 2670 | 2670 | 2670 |
| 52 | 185.2–186.9 | 2430 | 2385 | 2360 | 2335 | 2300 |
| 53 | 186.9–188.7 | 2155 | 2123 | 2114 | 2097 | 2079 |
| 54 | 188.7–190.5 | 1894 | 1871 | 1858 | 1843 | 1827 |
| 55 | 190.5–192.3 | 1612 | 1590 | 1577 | 1563 | 1548 |
| 56 | 192.3–194.2 | 1360 | 1339 | 1325 | 1312 | 1296 |
| 57 | 194.2–196.1 | 1118 | 1097 | 1081 | 1068 | 1052 |
| 58 | 196.1–198.0 | 905 | 882 | 865 | 851 | 834 |
| 59 | 198.0–200.0 | 712 | 689 | 671 | 656 | 638 |
| 60 | 200.0–202.0 | 552 | 528 | 510 | 494 | 477 |
| 61 | 202.0–204.1 | 422 | 398 | 380 | 365 | 348 |
| 62 | 204.1–206.2 | 313 | 291 | 274 | 260 | 244 |
| 63 | 206.2–208.3 | 229 | 209 | 194 | 181 | 167 |
| 64 | 208.3–210.5 | 163 | 145 | 132 | 121 | 110 |
| 65 | 210.5–212.8 | 114 | 99.3 | 88.7 | 79.7 | 71.0 |
| 66 | 212.8–215.0 | 77.6 | 65.7 | 57.4 | 50.5 | 44.0 |
| 67 | 215.0–217.4 | 52.1 | 42.9 | 36.6 | 31.4 | 26.8 |
| 68 | 217.4–219.8 | 34.0 | 27.1 | 22.6 | 18.9 | 15.7 |
| 69 | 219.8–222.2 | 21.8 | 16.9 | 13.8 | 11.3 | 9.15 |
| 70 | 222.2–224.7 | 13.9 | 10.5 | 8.33 | 6.66 | 5.30 |
| 71 | 224.7–227.3 | 8.42 | 6.16 | 4.79 | 3.73 | 2.91 |
| 72 | 227.3–229.9 | 5.00 | 3.60 | 2.77 | 2.12 | 1.64 |

Table IXa. $CHF_2Cl$

| λ (nm) | $\sigma(\lambda) \times 10^{21}$ ($cm^2$ $molec.^{-1}$) | | | | |
|---|---|---|---|---|---|
| | 295 K | 270 K | 250 K | 230 K | 210 K |
| 174 | 57.2 | 57.2 | 57.2 | 57.2 | 57.2 |
| 176 | 40.4 | 40.4 | 40.4 | 40.4 | 40.4 |
| 178 | 27.6 | 27.6 | 27.6 | 27.6 | 27.6 |
| 180 | 19.1 | 19.1 | 19.1 | 19.1 | 19.1 |
| 182 | 12.8 | 12.8 | 12.8 | 12.8 | 12.8 |
| 184 | 8.42 | 8.42 | 8.42 | 8.42 | 8.42 |
| 186 | 5.76 | 5.76 | 5.76 | 5.76 | 5.76 |
| 188 | 3.72 | 3.72 | 3.72 | 3.72 | 3.72 |
| 190 | 2.45 | 2.45 | 2.45 | 2.45 | 2.42 |
| 192 | 1.56 | 1.56 | 1.56 | 1.52 | 1.48 |
| 194 | 1.03 | 1.02 | 0.99 | 0.96 | 0.93 |
| 196 | 0.72 | 0.69 | 0.67 | 0.64 | 0.62 |
| 198 | 0.48 | 0.45 | 0.43 | 0.41 | 0.39 |
| 200 | 0.32 | 0.29 | 0.278 | 0.259 | 0.246 |
| 202 | 0.220 | 0.192 | 0.184 | 0.169 | 0.159 |
| 204 | 0.142 | 0.121 | 0.114 | 0.104 | 0.096 |

Table IXb. $CHF_2Cl$ (wavenumber intervals: 500 $cm^{-1}$)

| No. | $\lambda$ (nm) | $\sigma(\lambda) \times 10^{21}$ ($cm^2$ molec.$^{-1}$) | | | | |
|---|---|---|---|---|---|---|
| | | 295 K | 270 K | 250 K | 230 K | 210 K |
| 45 | 173.9–175.4 | 51.7 | 51.7 | 51.7 | 51.7 | 51.7 |
| 46 | 175.4–177.0 | 38.0 | 38.0 | 38.0 | 38.0 | 38.0 |
| 47 | 177.0–178.6 | 28.8 | 28.8 | 28.8 | 28.8 | 28.8 |
| 48 | 178.6–180.2 | 21.2 | 21.2 | 21.2 | 21.2 | 21.2 |
| 49 | 180.2–181.8 | 15.5 | 15.5 | 15.5 | 15.5 | 15.5 |
| 50 | 181.8–183.5 | 11.3 | 11.3 | 11.3 | 11.3 | 11.3 |
| 51 | 183.5–185.2 | 8.03 | 8.03 | 8.03 | 8.03 | 8.03 |
| 52 | 185.2–186.9 | 5.65 | 5.65 | 5.65 | 5.65 | 5.65 |
| 53 | 186.9–188.7 | 3.88 | 3.88 | 3.88 | 3.88 | 3.88 |
| 54 | 188.7–190.5 | 2.72 | 2.72 | 2.72 | 2.72 | 2.72 |
| 55 | 190.5–192.3 | 1.83 | 1.82 | 1.80 | 1.77 | 1.72 |
| 56 | 192.3–194.2 | 1.26 | 1.24 | 1.22 | 1.19 | 1.15 |
| 57 | 194.2–196.1 | 0.850 | 0.825 | 0.806 | 0.778 | 0.747 |
| 58 | 196.1–198.0 | 0.576 | 0.548 | 0.532 | 0.508 | 0.484 |
| 59 | 198.0–200.0 | 0.385 | 0.357 | 0.344 | 0.324 | 0.307 |
| 60 | 200.0–202.0 | 0.259 | 0.233 | 0.223 | 0.207 | 0.194 |
| 61 | 202.0–204.1 | 0.177 | 0.153 | 0.144 | 0.132 | 0.123 |

Table Xa. $CHFCl_2$

| $\lambda$ (nm) | $\sigma(\lambda) \times 10^{21}$ ($cm^2$ molec.$^{-1}$) | | | | |
|---|---|---|---|---|---|
| | 295 K | 270 K | 250 K | 230 K | 210 K |
| 174 | 1660 | 1660 | 1660 | 1660 | 1660 |
| 176 | 1645 | 1645 | 1645 | 1645 | 1645 |
| 178 | 1550 | 1550 | 1550 | 1550 | 1550 |
| 180 | 1380 | 1380 | 1380 | 1380 | 1380 |
| 182 | 1160 | 1160 | 1160 | 1160 | 1160 |
| 184 | 924 | 924 | 924 | 924 | 924 |
| 186 | 715 | 715 | 715 | 715 | 715 |
| 188 | 532 | 532 | 529 | 525 | 520 |
| 190 | 384 | 381 | 376 | 371 | 365 |
| 192 | 269 | 264 | 259 | 254 | 247 |
| 194 | 184 | 179 | 173 | 168 | 162 |
| 196 | 123 | 118 | 113 | 109 | 104 |
| 198 | 81.0 | 76.2 | 72.4 | 68.9 | 65.0 |
| 200 | 52.4 | 48.5 | 45.6 | 42.9 | 39.9 |
| 202 | 33.5 | 30.5 | 28.3 | 26.3 | 24.2 |
| 204 | 21.2 | 19.0 | 17.4 | 15.9 | 14.5 |
| 206 | 13.4 | 11.7 | 10.6 | 9.61 | 8.67 |
| 208 | 8.36 | 7.20 | 6.45 | 5.78 | 5.16 |
| 210 | 5.22 | 4.43 | 3.92 | 3.47 | 3.08 |
| 212 | 3.25 | 2.72 | 2.39 | 2.10 | 1.84 |
| 214 | 2.03 | 1.68 | 1.46 | 1.27 | 1.11 |
| 216 | 1.27 | 1.04 | 0.904 | 0.782 | 0.681 |
| 218 | 0.797 | 0.654 | 0.564 | 0.487 | 0.423 |
| 220 | 0.503 | 0.414 | 0.357 | 0.308 | 0.268 |
| 222 | 0.319 | 0.266 | 0.229 | 0.199 | 0.174 |

Table Xb. $CHFCl_2$ (wavenumber intervals: 500 $cm^{-1}$)

| No. | λ (nm) | σ(λ) × $10^{21}$ ($cm^2$ molec.$^{-1}$) | | | | |
|---|---|---|---|---|---|---|
| | | 295 K | 270 K | 250 K | 230 K | 210 K |
| 45 | 173.9–175.4 | 1660 | 1660 | 1660 | 1660 | 1660 |
| 46 | 175.4–177.0 | 1640 | 1640 | 1640 | 1640 | 1640 |
| 47 | 177.0–178.6 | 1565 | 1565 | 1565 | 1565 | 1565 |
| 48 | 178.6–180.2 | 1435 | 1435 | 1435 | 1435 | 1435 |
| 49 | 180.2–181.8 | 1270 | 1270 | 1270 | 1270 | 1270 |
| 50 | 181.8–183.5 | 1090 | 1090 | 1090 | 1090 | 1090 |
| 51 | 183.5–185.2 | 896 | 896 | 896 | 896 | 896 |
| 52 | 185.2–186.9 | 715 | 715 | 715 | 715 | 715 |
| 53 | 186.9–188.7 | 550 | 548 | 544 | 540 | 535 |
| 54 | 188.7–190.5 | 419 | 415 | 410 | 405 | 398 |
| 55 | 190.5–192.3 | 301 | 296 | 290 | 285 | 278 |
| 56 | 192.3–194.2 | 215 | 210 | 204 | 199 | 192 |
| 57 | 194.2–196.1 | 148 | 143 | 137 | 133 | 127 |
| 58 | 196.1–198.0 | 100 | 95.1 | 90.8 | 86.9 | 82.5 |
| 59 | 198.0–200.0 | 65.2 | 61.0 | 57.6 | 54.5 | 51.2 |
| 60 | 200.0–202.0 | 41.9 | 38.6 | 36.0 | 33.7 | 31.2 |
| 61 | 202.0–204.1 | 26.7 | 24.1 | 22.2 | 20.5 | 18.8 |
| 62 | 204.1–206.2 | 16.4 | 14.6 | 13.3 | 12.1 | 11.0 |
| 63 | 206.2–208.3 | 10.1 | 8.75 | 7.88 | 7.09 | 6.35 |
| 64 | 208.3–210.5 | 6.01 | 5.12 | 4.55 | 4.04 | 3.59 |
| 65 | 210.5–212.8 | 3.58 | 3.00 | 2.64 | 2.31 | 2.04 |
| 66 | 212.8–215.0 | 2.08 | 1.72 | 1.50 | 1.30 | 1.14 |
| 67 | 215.0–217.4 | 1.21 | 0.995 | 0.860 | 0.744 | 0.647 |
| 68 | 217.4–219.8 | 0.695 | 0.569 | 0.490 | 0.423 | 0.368 |

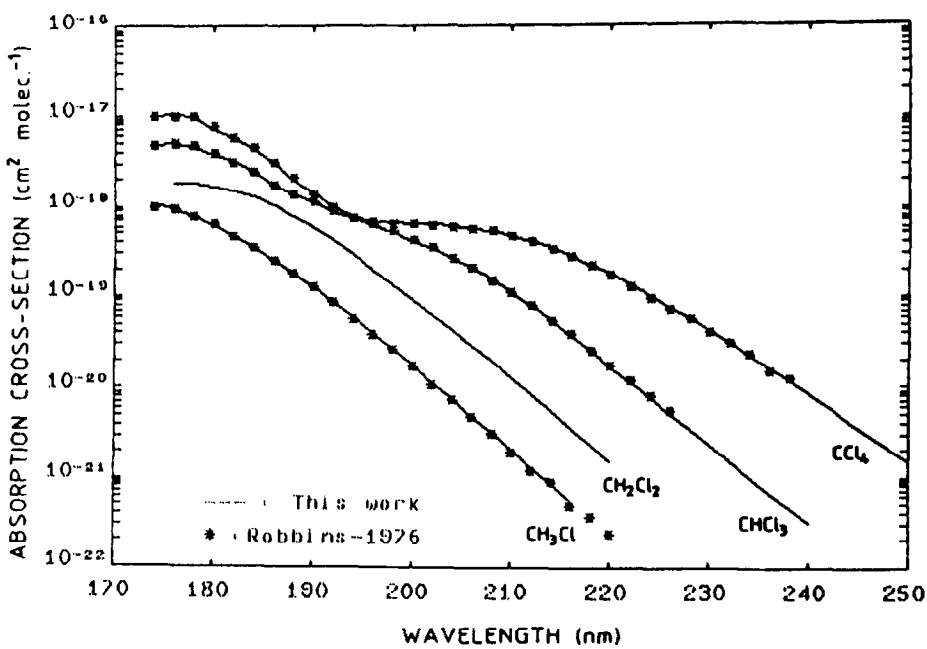


Fig. 1. Ultraviolet absorption cross-sections of $CH_3Cl$, $CH_2Cl_2$, $CHCl_3$, and $CCl_4$ with respect to wavelength at 295 K.

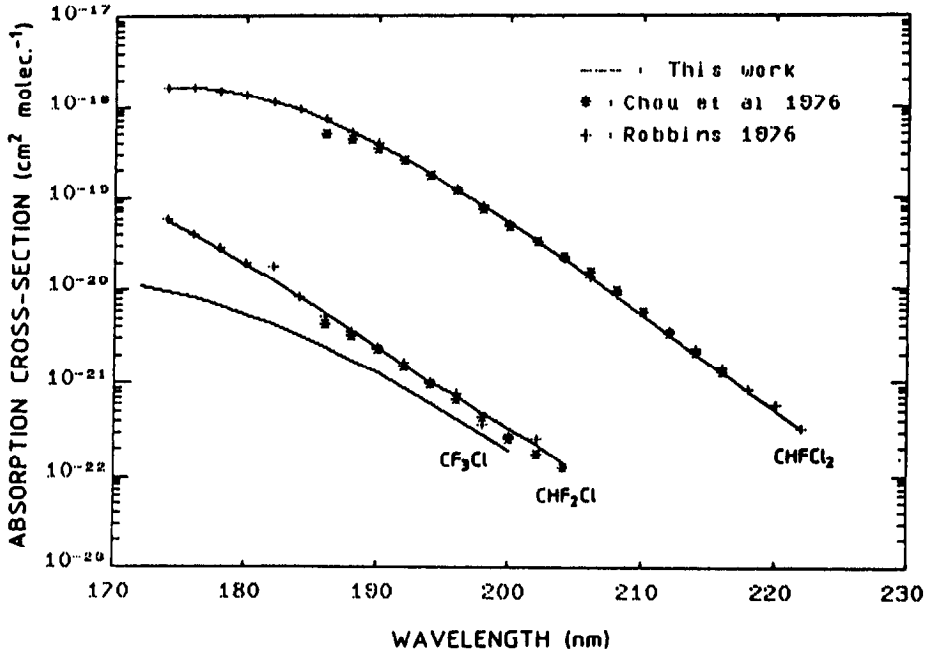


Fig. 2. Ultraviolet absorption cross-sections of $CF_3Cl$, $CF_2Cl_2$, $CFCl_3$, and $CCl_4$ with respect to wavelength at 295 K

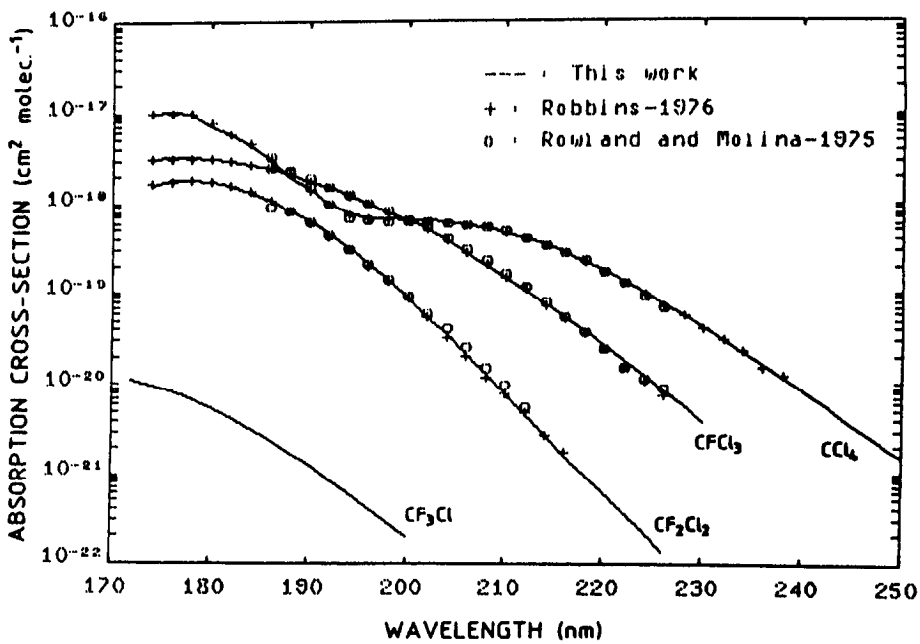


Fig. 3. Ultraviolet absorption cross-sections of $CF_3Cl$, $CHF_2Cl$, and $CHFCl_2$ with respect to wavelength at 295 K.

negligible compared to the stratospheric contribution; even in the case of the most absorbing compound ($CCl_4$), the absorption cross-section does not exceed $10^{-26}$ cm$^2$ molec.$^{-1}$ in the 300 nm region (Rebbert and Ausloos, 1976).

### 3.2. LOW TEMPERATURE (225–270 K)

For each compound, absorption cross-sections have been measured for different temperatures in the largest range afforded by vapor pressure conditions which limit the maximum working pressure. The actual experimental conditions are summarized in Table XI.

As shown in Figures 4–6, absorption cross-sections decrease with temperature by a factor which depends on both the wavelength and the chemical composition of the compound. This effect is most significant at low temperatures and in spectral regions of low absorptions. The temperature dependence is more important in the case of highly chlorinated substances, but vanishes progressively in the region of higher absorptions. Temperature effect, if any, was too small to be detected in our experimental conditions in the case of $CF_3Cl$.

For all compounds, the relationship between the absorption cross-sections and the temperature for a given wavelength is characterized by an exponential decrease depending upon wavelength and temperature values (295, 270, 255, and 255 K). Consequently, extrapolation based on four temperatures well distributed within the temperature range, can easily be made down to 210 K within the accuracy range defined above.

Numerical values are presented in Tables II–X for selected temperatures (270, 250, 230, 210 K) which cover the usual stratospheric conditions.

Similar measurements have previously been made only at two temperatures, 296 and 223 K, in the particular case of $CF_2Cl_2$ and $CFCl_3$, by Bass and Ledford (1976) who used optical paths up to 10 m and by Chou *et al.* (1977) with a 10 cm absorption cell at several temperatures between 212 and 296 K. Comparison with the available data is given on Figures 7, 8, and 9.

For $CF_2Cl_2$, values reported in this work confirm the previous results of Bass and Ledford (1976), down to 215 nm. The results published by Chou *et al.* (1977), give systematically higher values than those reported by Bass and Ledford and in this work. At 220 nm

Table XI. Experimental conditions for the measurement of absorption cross-sections at low temperatures

| | Temperature range (K) | Max. working pressure[a] (torr) | Wavelength range showing $T$ (dependence) (nm) |
|---|---|---|---|
| $CH_3Cl$ | 295–225 | 20 | 198–216 |
| $CH_2Cl_2$ | 295–225 | 3 | 192–220 |
| $CHCl_3$ | 295–230 | 2 | 194–230 |
| $CCl_4$ | 295–225 | 4 | 204–250 |
| $CF_3Cl$ | 295–225 | 700 | – |
| $CF_2Cl_2$ | 295–225 | 25 | 188–220 |
| $CFCl_3$ | 295–225 | 5 | 186–230 |
| $CHF_2Cl$ | 295–225 | 40 | 192–204 |
| $CHFCl_2$ | 295–225 | 7 | 188–222 |

[a] At the lowest working temperature.

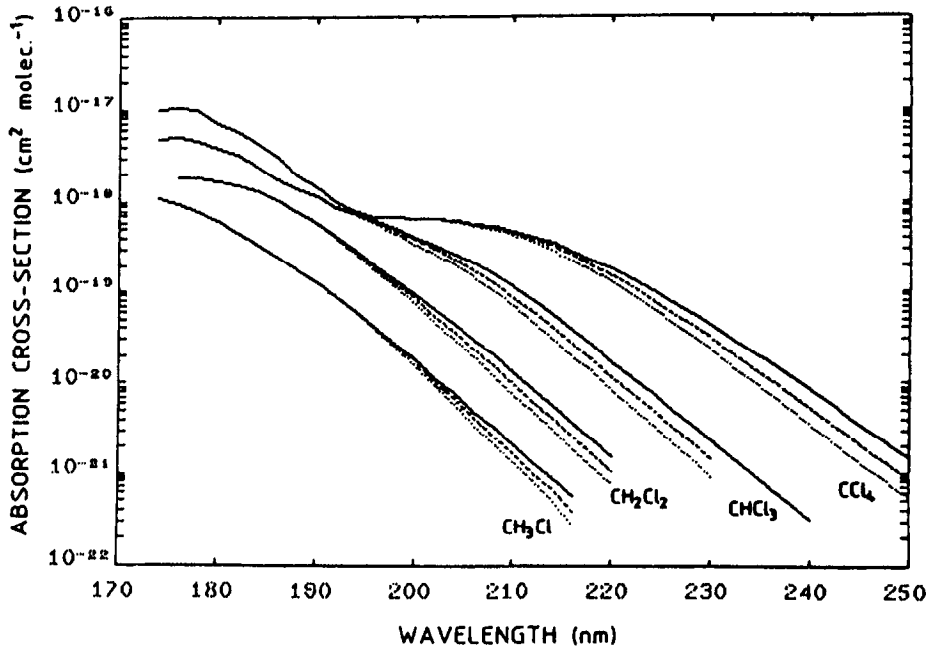


Fig. 4. Ultraviolet absorption cross-sections of $CH_3Cl$, $CH_2Cl_2$, $CHCl_3$, and $CCl_4$ versus wavelength as a function of temperature. 295 K: ———, 250 K: – – –, 210 K: . . . . .

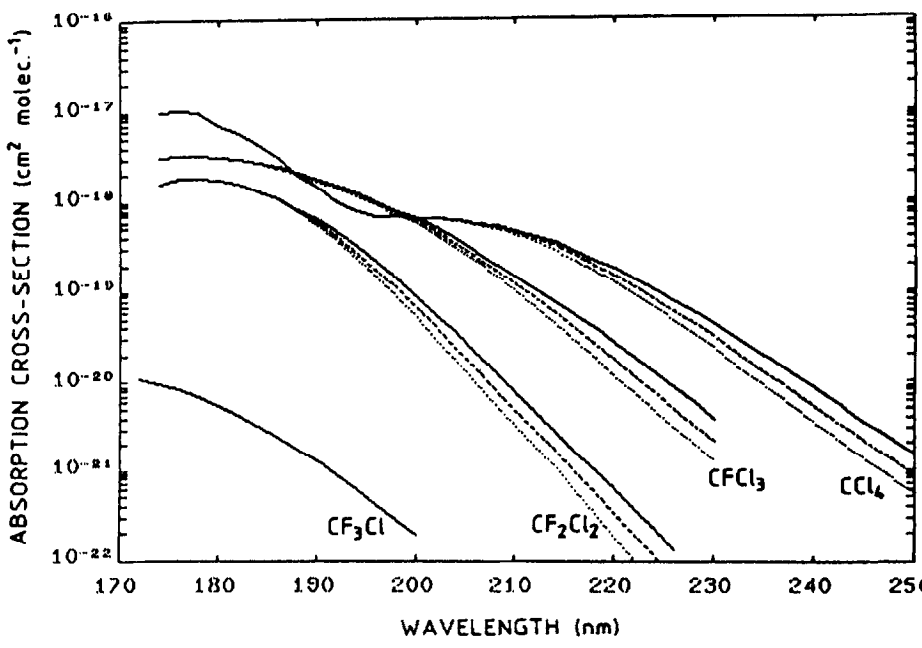


Fig. 5. Ultraviolet absorption cross-sections of $CF_3Cl$, $CF_2Cl_2$, $CFCl_3$, and $CCl_4$ versus wavelength as a function of temperature. 295 K: ———, 250 K: – – –, 210 K: . . . . .

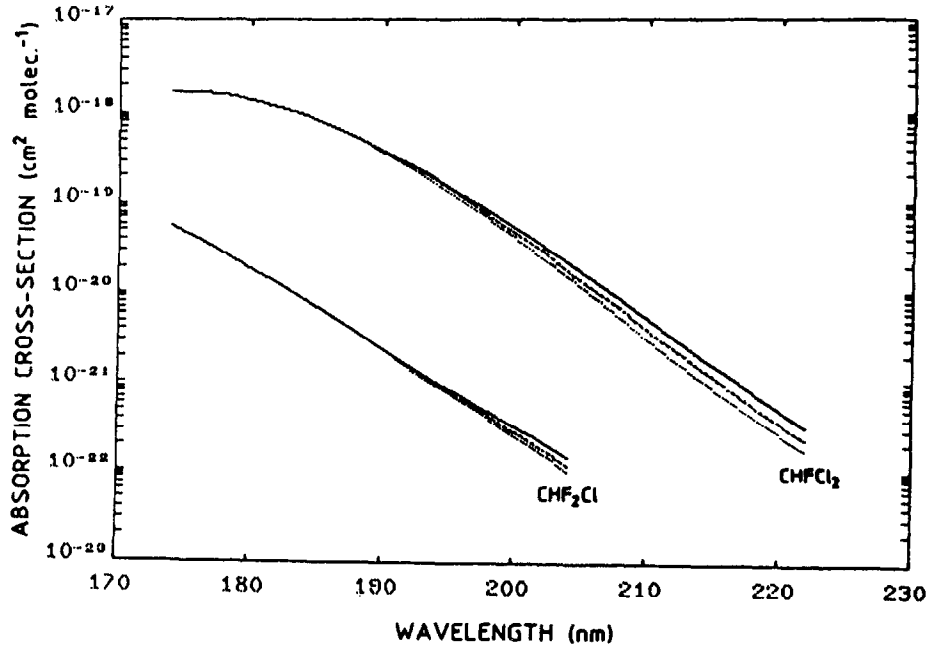


Fig. 6. Ultraviolet absorption cross-sections of $CHF_2Cl$ and $CHFCl_2$ versus wavelength as a function of temperature. 295 K: ———, 250 K: – – –, 210 K: . . . . .

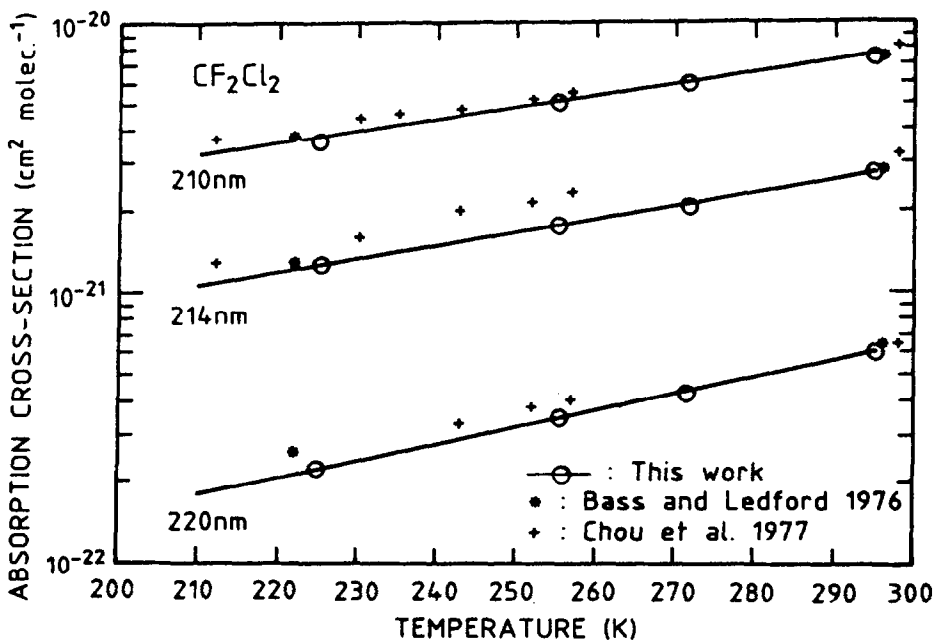


Fig. 7. Absorption cross-sections of $CF_2Cl_2$ versus temperature at three wavelengths (210, 214, and 220 nm).

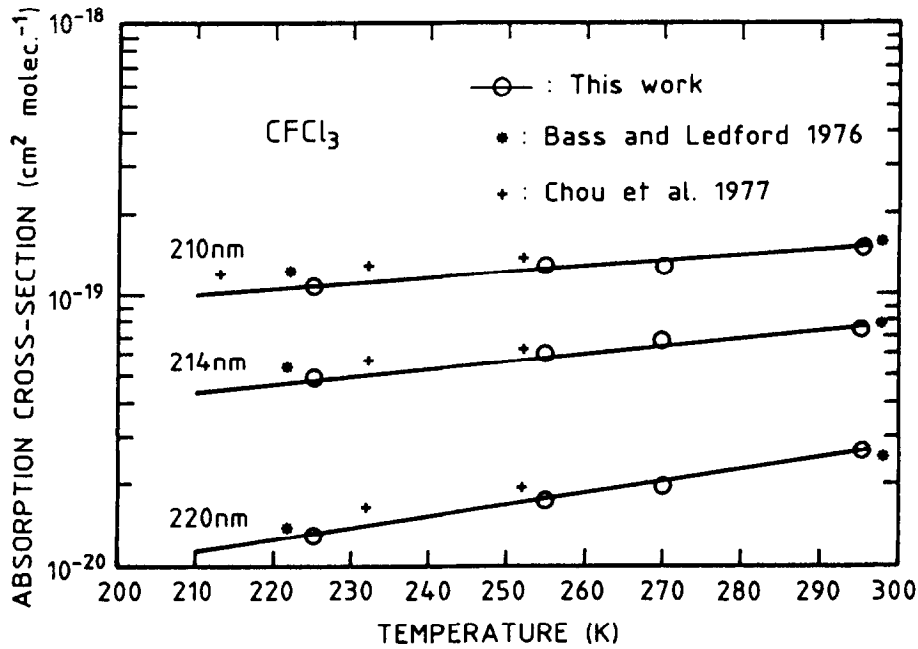


Fig. 8. Absorption cross-sections of $CFCl_3$ versus temperature at three wavelengths (210, 214 and 220 nm).

where the absorption cross-sections are below $10^{-21}$ cm$^2$ molec.$^{-1}$, the agreement between Bass and Ledford and Chou *et al.* seems better, but both give higher values and, consequently, a less pronounced temperature dependence. Actually, this wavelength represents the lower limit in the measurements given by both authors.

A similar conclusion can be drawn from Figure 8 giving the comparison between measurements performed for $CFCl_3$ and can be extended down to 200 nm.

Absorption cross-sections for $CH_3Cl$, $CFCl_3$, $CF_2Cl_2$, $CHF_2Cl$, and $CHFCl_2$ have also been published by Hubrich *et al.* (1977) and Hubrich and Stuhl (1980) for only one low temperature (208 K). Their results confirm qualitatively the general conclusions mentioned above and are in fairly good agreement for $CF_2Cl_2$ between 190 and 205 nm (within the experimental accuracy of 4%) but diverge from about $-5\%$ at 200 nm up to $\pm 40\%$ at 230 nm for $CFCl_3$.

For the other compounds, differences of more than 20% are observed with their values, even at room temperature.

Discrepancies can be explained by a critical analysis of the experimental conditions reported by Hubrich *et al.* (1977) and Hubrich and Stuhl (1980) which reveals that some measurements have been performed in less favorable conditions, namely transmitted fluxes lower than 5% or higher than 95%, leading to larger uncertainties than those reported in this work for which experimental measurements for transmission below 10% and above 85% have been eliminated in order to stay in a range where the Beer-Lambert law is applicable within the quoted accuracy.

As explained above, the absorption cross-sections can be represented by an empirical function of temperature for each wavelength, according to the following expression

$$\log 10\, \sigma(\lambda) = A(\lambda) + B(\lambda) \times T, \tag{2}$$

where the parameters $A$ and $B$ were determined by a polynomial fitting of the available

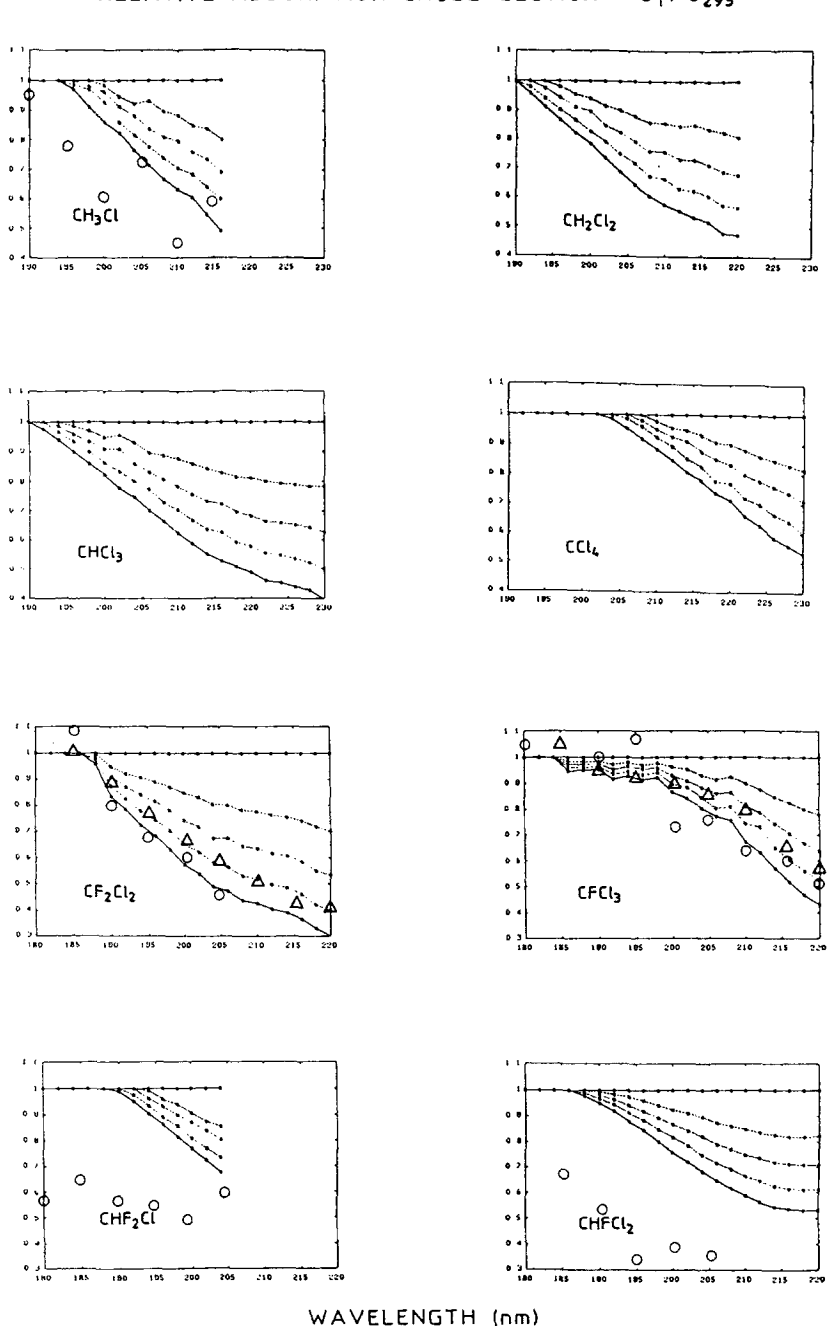


Fig. 9. Relative absorption cross-sections $\sigma(T)/\sigma(295\text{ K})$ as a function of wavelength for the eight chlorofluoromethanes showing a temperature dependence. -*-: this work ($T = 270$ K, 250 K, 230 K and 210 K), △: Bass and Ledford (1976) ($T = 223$ K), ○: Hubrich *et al.* (1977) ($T = 208$ K). Note: values from Chou *et al.* (1978) are not plotted on this figure for sake of clarity.

Table XII. Parameters A and B for polynomial function (see formula (3) in the text)

| | |
|---|---|
| *$CH_3Cl$:* | |
| $A_0 = -299.80$ | $B_0 = -7.1727$ |
| $A_1 = 5.1047$ | $B_1 = 1.4837\ 10^{-1}$ |
| $A_2 = -3.3630\ 10^{-2}$ | $B_2 = -1.1463\ 10^{-3}$ |
| $A_3 = 9.5805\ 10^{-5}$ | $B_3 = 3.9188\ 10^{-6}$ |
| $A_4 = -1.0135\ 10^{-7}$ | $B_4 = -4.9994\ 10^{-9}$ |
| $T$ range: 210–300 K | |
| $\lambda$ range: 174–216 nm | |
| *$CH_2Cl_2$:* | |
| $A_0 = -1431.8$ | $B_0 = -3.1171$ |
| $A_1 = 27.395$ | $B_1 = 6.7874\ 10^{-2}$ |
| $A_2 = -1.9807\ 10^{-1}$ | $B_2 = -5.5000\ 10^{-4}$ |
| $A_3 = 6.3468\ 10^{-4}$ | $B_3 = 1.9649\ 10^{-6}$ |
| $A_4 = -7.6298\ 10^{-7}$ | $B_4 = -2.6101\ 10^{-9}$ |
| $T$ range: 210–300 K | |
| $\lambda$ range: 176–220 nm | |
| *$CHCl_3$:* | |
| $A_0 = 269.80$ | $B_0 = 3.7973$ |
| $A_1 = -6.0908$ | $B_1 = -7.0913\ 10^{-2}$ |
| $A_2 = 4.7830\ 10^{-2}$ | $B_2 = 4.9397\ 10^{-4}$ |
| $A_3 = -1.6427\ 10^{-4}$ | $B_3 = -1.5226\ 10^{-6}$ |
| $A_4 = 2.0682\ 10^{-7}$ | $B_4 = 1.7555\ 10^{-9}$ |
| $T$ range: 210–300 K | |
| $\lambda$ range: 190–240 nm | |
| *$CCl_4$:* | |
| $A_0 = -37.104$ | $B_0 = 1.0739$ |
| $A_1 = -5.8218\ 10^{-1}$ | $B_1 = -1.6275\ 10^{-2}$ |
| $A_2 = 9.9974\ 10^{-3}$ | $B_2 = 8.8141\ 10^{-5}$ |
| $A_3 = -4.6765\ 10^{-5}$ | $B_3 = -1.9811\ 10^{-7}$ |
| $A_4 = 6.8501\ 10^{-8}$ | $B_4 = 1.5022\ 10^{-10}$ |
| $T$ range: 210–300 K | |
| $\lambda$ range: 194–250 nm | |
| *$CF_3Cl$:* | |
| $A_0 = -155.88$ | $B_0 = 0$ |
| $A_1 = 2.0993$ | $B_1 = 0$ |
| $A_2 = -1.0486\ 10^{-2}$ | $B_2 = 0$ |
| $A_3 = 1.6718\ 10^{-5}$ | $B_3 = 0$ |
| $T$ range: 210–300 K | |
| $\lambda$ range: 172–220 nm | |
| *$CF_2Cl_2$:* | |
| $A_0 = -711.02$ | $B_0 = 6.1648$ |
| $A_1 = 12.490$ | $B_1 = -1.2093\ 10^{-1}$ |
| $A_2 = -8.2865\ 10^{-2}$ | $B_2 = 8.8587\ 10^{-4}$ |
| $A_3 = 2.4091\ 10^{-4}$ | $B_3 = -2.8743\ 10^{-6}$ |
| $A_4 = -2.6113\ 10^{-7}$ | $B_4 = 3.4904\ 10^{-9}$ |
| $T$ range: 210–300 K | |
| $\lambda$ range: 174–226 nm | |

Table XII. (*Continued*)

| | |
|---|---|
| *$CFCl_3$:* | |
| $A_1 = -84.611$ | $B_0 = -5.7912$ |
| $A_1 = 7.9551\ 10^{-1}$ | $B_1 = 1.1689\ 10^{-1}$ |
| $A_2 = -2.0550\ 10^{-3}$ | $B_2 = -8.8069\ 10^{-4}$ |
| $A_3 = -4.4812\ 10^{-6}$ | $B_3 = 2.9335\ 10^{-6}$ |
| $A_4 = 1.5838\ 10^{-8}$ | $B_4 = -3.6421\ 10^{-9}$ |
| $T$ range: 210–300 K | |
| $\lambda$ range: 174–230 nm | |
| *$CHF_2Cl$:* | |
| $A_0 = -106.029$ | $B_0 = -1.3399\ 10^{-1}$ |
| $A_1 = 1.5038$ | $B_1 = 2.7405\ 10^{-3}$ |
| $A_2 = -8.2476\ 10^{-3}$ | $B_2 = -1.8028\ 10^{-5}$ |
| $A_3 = 1.4206\ 10^{-5}$ | $B_3 = 3.8504\ 10^{-8}$ |
| $T$ range: 210–300 K | |
| $\lambda$ range: 174–204 nm | |
| *$CHFCl_2$:* | |
| $A_0 = -514.56$ | $B_0 = -3.0577$ |
| $A_1 = 8.7940$ | $B_1 = 6.6539\ 10^{-2}$ |
| $A_2 = -5.6840\ 10^{-2}$ | $B_2 = -5.3964\ 10^{-4}$ |
| $A_3 = 1.5894\ 10^{-4}$ | $B_3 = 1.9322\ 10^{-6}$ |
| $A_4 = -1.6345\ 10^{-7}$ | $B_4 = -2.5754\ 10^{-9}$ |
| $T$ range: 210–300 K | |
| $\lambda$ range: 174–222 nm | |

experimental data with respect to temperature and wavelength by means of a least-squares fit algorithm developed by The Math Works Inc. (PC. MATLAB) to obtain the following polynomial expression

$$\log_{10} \sigma(\lambda, T) = A_0 + A_1\lambda + \cdots + A_n\lambda^n + (T273) \times (B_0 + B_1\lambda + \cdots + B_n\lambda^n). \quad (3)$$

The computed values of the $A$ and $B$ parameters are given in Table XII.

The computed values of absorptions cross-sections calculated with expression (3) represent all the experimental data with differences lower than $\pm 4\%$.

## 4. Discussion

As discussed by Majer and Simons (1964) and Sandorfy (1976), the continuous absorption of chloro- and chlorofluoromethanes in the 200 nm region corresponds to the less energetic band of their electronic spectrum. It is due to the existence of a (C—Cl)* ← Cl transition involving excitation to a repulsive electronic state (C—Cl antibonding). Substitution of hydrogen atoms in the basic hydrocarbon entity by chlorine atoms leads to an increased absorption and a red shift of the average wavelength absorption range, while fluorine atoms play an opposite role and stabilize the molecule.

Unfortunately, the complexity of the spectrum features, especially in the case of polychloro-compounds, makes a theoretical analysis of temperature dependence of their absorption cross-sections very difficult.

Relative values of absorption cross-sections $\sigma(T)/\sigma(295)$ versus wavelength relationships, for a given temperature, display very similar features for all highly chlorinated compounds ($CH_2Cl_2$, $CHFCl_2$, $CHCl_3$, $CFCl_3$, $CCl_4$) while a greater specificity with the chemical composition is observed in the case of $CH_3Cl$, $CHF_2Cl$, $CF_3Cl$, and $CF_2Cl_2$ (Figure 9).

It is currently admitted in the wavelength and pressures ranges of stratospheric interest, that the most important process for the photodissociation of all the halocarbons is the release of one Cl atom with a unitary quantum yield, according to the general scheme

$$RCl_x \rightarrow RCl_{x-1} + Cl \tag{4}$$

The immediate reaction of $RCl_{x-1}$ with atmospheric $O_2$ releases another Cl atom, leaving $RCl_{x-2}$ which, in turn, can be subject to photolysis.

The ultimate fate of such radicals in stratospheric conditions ought to be considered in detail in order to define the production of ClO radicals due to the photodissociation of each halocarbons.

Photodissociation coefficients $J$ for a given altitude $z$, zenith angle $x$, and wavelength interval have been computed according to the relations

$$J^z = \sigma_\lambda q_\lambda(z),$$

$$q_\lambda(z) = q_\lambda(\infty)\, e^{-\tau_\lambda(z)}$$

$$\tau_\lambda(z) = \int_z^\infty [n(O_2)\sigma(O_2) + n(O_3)\sigma(O_3) + n(\text{air})\sigma_{\text{scatt.}}] \sec\chi \, dz,$$

where $\sigma$ is the absorption cross-section, $q_\lambda(z)$ and $q_\lambda(\infty)$ are the solar irradiance at altitude $z$ or extraterrestrial ($z = \infty$), and $n$ is the number of particles per volume unit, for solar zenith angles of 0° and 60° ($\sec\chi = 1$ and 2), taking the values of $\sigma(O_2)$, $\sigma(O_3)$ from WMO (1985) and Kockarts (1976), of $\sigma_{\text{scatt}}$ from Nicolet (1984) and the values of $q(\infty)$ from WMO (1985), and taking into account the actual values of the cross-sections which correspond to the temperature conditions prevailing at a definite altitude (Tables XIII and XIV, Figures 10 and 11).

A comparison of either temperature-dependent or independent photodissociation coefficients for different stratospheric altitudes (15 to 50 km) is presented in Table XIV, where relative photodissociation coefficients $J(T)/J(295)$ are given for all studied compounds. Obviously, the effect is maximum at low altitudes and gradually decreases, following the temperature profile in the stratosphere.

Table XIII. Temperature model

| Altitude (km) | Temperature (K) |
|---|---|
| 15 | 217 |
| 20 | 217 |
| 25 | 222 |
| 30 | 227 |
| 35 | 237 |
| 40 | 251 |
| 45 | 265 |
| 50 | 271 |

Table XIV. Photodissociation coefficients versus altitude

| $Z$ (km) | sec $\chi = 1$ | | $J_{rel}$ | sec $\chi = 2$ | | $J_{rel}$ |
|---|---|---|---|---|---|---|
| | $J(s^{-1})$ $\sigma$ (295 K)[a] | $J(s^{-1})$ $\sigma = f(T)$ | | $J(s^{-1})$ $\sigma$ (295 K)[a] | $J(s^{-1})$ $\sigma = f(T)$ | |
| *$CH_3Cl$:* | | | | | | |
| 15 | $1.063\ 10^{-10}$ | $7.837\ 10^{-11}$ | 0.737 | $2.686\ 10^{-13}$ | $2.003\ 10^{-13}$ | 0.746 |
| 20 | $1.412\ 10^{-9}$ | $1.094\ 10^{-9}$ | 0.775 | $2.548\ 10^{-11}$ | $1.932\ 10^{-11}$ | 0.758 |
| 25 | $9.471\ 10^{-9}$ | $7.895\ 10^{-9}$ | 0.834 | $6.526\ 10^{-10}$ | $5.342\ 10^{-10}$ | 0.818 |
| 30 | $3.917\ 10^{-8}$ | $3.414\ 10^{-8}$ | 0.872 | $7.206\ 10^{-9}$ | $6.095\ 10^{-9}$ | 0.846 |
| 35 | $1.095\ 10^{-7}$ | $9.982\ 10^{-8}$ | 0.912 | $3.962\ 10^{-8}$ | $3.527\ 10^{-8}$ | 0.890 |
| 40 | $2.196\ 10^{-7}$ | $2.075\ 10^{-7}$ | 0.945 | $1.219\ 10^{-7}$ | $1.134\ 10^{-7}$ | 0.930 |
| 45 | $3.346\ 10^{-7}$ | $3.244\ 10^{-7}$ | 0.969 | $2.277\ 10^{-7}$ | $2.188\ 10^{-7}$ | 0.961 |
| 50 | $4.444\ 10^{-7}$ | $4.354\ 10^{-7}$ | 0.980 | $3.314\ 10^{-7}$ | $3.230\ 10^{-7}$ | 0.975 |
| *$CH_2Cl_2$:* | | | | | | |
| 15 | $6.225\ 10^{-10}$ | $4.134\ 10^{-10}$ | 0.644 | $1.564\ 10^{-12}$ | $1.049\ 10^{-12}$ | 0.671 |
| 20 | $8.080\ 10^{-9}$ | $5.620\ 10^{-9}$ | 0.696 | $1.472\ 10^{-10}$ | $1.003\ 10^{-10}$ | 0.681 |
| 25 | $5.269\ 10^{-8}$ | $3.945\ 10^{-8}$ | 0.749 | $3.694\ 10^{-9}$ | $2.680\ 10^{-9}$ | 0.725 |
| 30 | $2.121\ 10^{-7}$ | $1.688\ 10^{-7}$ | 0.796 | $3.988\ 10^{-8}$ | $3.068\ 10^{-8}$ | 0.769 |
| 35 | $5.784\ 10^{-7}$ | $4.899\ 10^{-7}$ | 0.846 | $2.146\ 10^{-7}$ | $1.766\ 10^{-7}$ | 0.823 |
| 40 | $1.131\ 10^{-6}$ | $1.014\ 10^{-6}$ | 0.896 | $6.474\ 10^{-7}$ | $5.680\ 10^{-7}$ | 0.877 |
| 45 | $1.673\ 10^{-6}$ | $1.569\ 10^{-6}$ | 0.938 | $1.180\ 10^{-6}$ | $1.091\ 10^{-6}$ | 0.925 |
| 50 | $2.149\ 10^{-6}$ | $2.055\ 10^{-6}$ | 0.956 | $1.665\ 10^{-6}$ | $1.577\ 10^{-6}$ | 0.947 |
| *$CHCl_3$:* | | | | | | |
| 15 | $4.521\ 10^{-9}$ | $3.179\ 10^{-9}$ | 0.701 | $1.117\ 10^{-11}$ | $7.948\ 10^{-12}$ | 0.712 |
| 20 | $5.325\ 10^{-8}$ | $3.838\ 10^{-8}$ | 0.721 | $1.017\ 10^{-9}$ | $7.298\ 10^{-10}$ | 0.718 |
| 25 | $3.062\ 10^{-7}$ | $2\text{-}318\ 10^{-7}$ | 0.757 | $2.323\ 10^{-8}$ | $1.741\ 10^{-8}$ | 0.749 |
| 30 | $1.094\ 10^{-6}$ | $8.601\ 10^{-7}$ | 0.786 | $2.264\ 10^{-7}$ | $1.761\ 10^{-7}$ | 0.778 |
| 35 | $2.704\ 10^{-6}$ | $2.222\ 10^{-6}$ | 0.822 | $1.108\ 10^{-6}$ | $9.024\ 10^{-7}$ | 0.814 |
| 40 | $4.921\ 10^{-6}$ | $4.261\ 10^{-6}$ | 0.866 | $3.107\ 10^{-6}$ | $2.657\ 10^{-6}$ | 0.855 |
| 45 | $6.773\ 10^{-6}$ | $6.132\ 10^{-6}$ | 0.905 | $5.294\ 10^{-6}$ | $4.755\ 10^{-6}$ | 0.898 |
| 50 | $8.050\ 10^{-6}$ | $7.457\ 10^{-6}$ | 0.926 | $6.878\ 10^{-6}$ | $6.327\ 10^{-6}$ | 0.920 |
| *$CCl_4$:* | | | | | | |
| 15 | $1.490\ 10^{-8}$ | $1.387\ 10^{-8}$ | 0.930 | $3.381\ 10^{-11}$ | $3.200\ 10^{-11}$ | 0.946 |
| 20 | $1.630\ 10^{-7}$ | $1.523\ 10^{-7}$ | 0.934 | $3.020\ 10^{-9}$ | $2.857\ 10^{-9}$ | 0.946 |
| 25 | $8.752\ 10^{-7}$ | $8.206\ 10^{-7}$ | 0.938 | $6.520\ 10^{-8}$ | $6.194\ 10^{-8}$ | 0.950 |
| 30 | $3.075\ 10^{-6}$ | $2.870\ 10^{-6}$ | 0.933 | $6.169\ 10^{-7}$ | $5.850\ 10^{-7}$ | 0.948 |
| 35 | $7.950\ 10^{-6}$ | $7.368\ 10^{-6}$ | 0.927 | $3.121\ 10^{-6}$ | $2.942\ 10^{-6}$ | 0.943 |
| 40 | $1.593\ 10^{-5}$ | $1.471\ 10^{-5}$ | 0.924 | $9.748\ 10^{-6}$ | $9.121\ 10^{-6}$ | 0.936 |
| 45 | $2.331\ 10^{-5}$ | $2\text{-}181\ 10^{-5}$ | 0.936 | $1.835\ 10^{-5}$ | $1.725\ 10^{-5}$ | 0.940 |
| 50 | $2.774\ 10^{-5}$ | $2.618\ 10^{-5}$ | 0.944 | $2.454\ 10^{-5}$ | $2.316\ 10^{-5}$ | 0.944 |
| *$CF_3Cl$:* | | | | | | |
| 15 | $4.579\ 10^{-14}$ | | | $6.410\ 10^{-18}$ | | |
| 20 | $3.380\ 10^{-12}$ | | | $1.976\ 10^{-14}$ | | |
| 25 | $4.341\ 10^{-11}$ | | | $1.892\ 10^{-12}$ | | |
| 30 | $2.385\ 10^{-10}$ | | | $3.462\ 10^{-11}$ | | |
| 35 | $7.700\ 10^{-10}$ | | | $2.412\ 10^{-10}$ | | |
| 40 | $1.675\ 10^{-9}$ | | | $8.444\ 10^{-10}$ | | |
| 45 | $2.690\ 10^{-9}$ | | | $1.717\ 10^{-9}$ | | |
| 50 | $3.701\ 10^{-9}$ | | | $2.647\ 10^{-9}$ | | |

Table XIV. (*Continued*)

| $Z$ (km) | sec $\chi = 1$ | | $J_{rel}$ | sec $\chi = 2$ | | $J_{rel}$ |
|---|---|---|---|---|---|---|
| | $J(s^{-1})$ $\sigma$ (295 K)[a] | $J(s^{-1})$ $\sigma = f(T)$ | | $J(s^{-1})$ $\sigma$ (295 K)[a] | $J(s^{-1})$ $\sigma = f(T)$ | |
| *$CF_2Cl_2$:* | | | | | | |
| 15 | $4.447\ 10^{-10}$ | $2.253\ 10^{-10}$ | 0.503 | $1.146\ 10^{-12}$ | $5.789\ 10^{-13}$ | 0.505 |
| 20 | $6.238\ 10^{-9}$ | $3.345\ 10^{-9}$ | 0.536 | $1.105\ 10^{-10}$ | $5.704\ 10^{-11}$ | 0.516 |
| 25 | $4.385\ 10^{-8}$ | $2.628\ 10^{-8}$ | 0.599 | $2.946\ 10^{-9}$ | $1.674\ 10^{-9}$ | 0.568 |
| 30 | $1.867\ 10^{-7}$ | $1.235\ 10^{-7}$ | 0.662 | $3.364\ 10^{-8}$ | $2.101\ 10^{-8}$ | 0.625 |
| 35 | $5.297\ 10^{-7}$ | $3.909\ 10^{-7}$ | 0.738 | $1.889\ 10^{-7}$ | $1.329\ 10^{-7}$ | 0.703 |
| 40 | $1.065\ 10^{-6}$ | $8.698\ 10^{-7}$ | 0.817 | $5.886\ 10^{-7}$ | $4.651\ 10^{-7}$ | 0.790 |
| 45 | $1.610\ 10^{-6}$ | $1.425\ 10^{-6}$ | 0.885 | $1.105\ 10^{-6}$ | $9.584\ 10^{-7}$ | 0.867 |
| 50 | $2.099\ 10^{-6}$ | $1.92.\ 10^{-6}$ | 0.917 | $1.597\ 10^{-6}$ | $1.443\ 10^{-6}$ | 0.903 |
| *$CFCl_3$:* | | | | | | |
| 15 | $6.240\ 10^{-9}$ | $4.701\ 10^{-9}$ | 0.753 | $1.532\ 10^{-11}$ | $1.178\ 10^{-11}$ | 0.769 |
| 20 | $7.480\ 10^{-8}$ | $5.797\ 10^{-8}$ | 0.775 | $1.406\ 10^{-9}$ | $1.090\ 10^{-9}$ | 0.775 |
| 25 | $4.403\ 10^{-7}$ | $3.557\ 10^{-7}$ | 0.808 | $3.278\ 10^{-8}$ | $2.636\ 10^{-8}$ | 0.804 |
| 30 | $1.607\ 10^{-6}$ | $1.334\ 10^{-6}$ | 0.830 | $3.263\ 10^{-7}$ | $2.701\ 10^{-7}$ | 0.828 |
| 35 | $4{,}033\ 10^{-6}$ | $3.443\ 10^{-6}$ | 0.854 | $1.627\ 10^{-6}$ | $1.388\ 10^{-6}$ | 0.853 |
| 40 | $7.408\ 10^{-6}$ | $6.525\ 10^{-6}$ | 0.881 | $4.631\ 10^{-6}$ | $4.070\ 10^{-6}$ | 0.879 |
| 45 | $1.021\ 10^{-5}$ | $9.342\ 10^{-6}$ | 0.915 | $7.963\ 10^{-6}$ | $7.253\ 10^{-6}$ | 0.911 |
| 50 | $1.206\ 10^{-5}$ | $1.125\ 10^{-5}$ | 0.932 | $1.037\ 10^{-5}$ | $9.618\ 10^{-6}$ | 0.927 |
| *$CHF_2Cl$:* | | | | | | |
| 15 | $1.944\ 10^{-13}$ | $1.449\ 10^{-13}$ | 0.727 | $5.261\ 10^{-17}$ | $3.865\ 10^{-17}$ | 0.735 |
| 20 | $9.692\ 10^{-12}$ | $7.416\ 10^{-12}$ | 0.765 | $7.935\ 10^{-14}$ | $5.926\ 10^{-14}$ | 0.747 |
| 25 | $1.020\ 10^{-10}$ | $8.196\ 10^{-11}$ | 0.803 | $5.363\ 10^{-12}$ | $4.177\ 10^{-12}$ | 0.779 |
| 30 | $5.053\ 10^{-10}$ | $4.262\ 10^{-10}$ | 0.844 | $8.131\ 10^{-11}$ | $6.629\ 10^{-11}$ | 0.815 |
| 35 | $1.558\ 10^{-9}$ | $1.386\ 10^{-9}$ | 0.889 | $5.108\ 10^{-10}$ | $4.421\ 10^{-10}$ | 0.866 |
| 40 | $3.360\ 10^{-9}$ | $3.126\ 10^{-9}$ | 0.930 | $1.708\ 10^{-9}$ | $1.562\ 10^{-9}$ | 0.915 |
| 45 | $5.471\ 10^{-9}$ | $2.256\ 10^{-9}$ | 0.961 | $3.441\ 10^{-9}$ | $3.272\ 10^{-9}$ | 0.951 |
| 50 | $7.743\ 10^{-9}$ | $7.541\ 10^{-9}$ | 0.974 | $5.369\ 10^{-9}$ | $5.192\ 10^{-9}$ | 0.967 |
| *$CHFCl_2$:* | | | | | | |
| 15 | $2.884\ 10^{-10}$ | $1.932\ 10^{-10}$ | 0.670 | $7.330\ 10^{-13}$ | $4.936\ 10^{-13}$ | 0.673 |
| 20 | $3.929\ 10^{-9}$ | $2.756\ 10^{-9}$ | 0.701 | $7.015\ 10^{-11}$ | $4.798\ 10^{-11}$ | 0.684 |
| 25 | $2.706\ 10^{-8}$ | $2.041\ 10^{-8}$ | 0.754 | $1.836\ 10^{-9}$ | $1.338\ 10^{-9}$ | 0.728 |
| 30 | $1.140\ 10^{-7}$ | $9.145\ 10^{-8}$ | 0.802 | $2.068\ 10^{-8}$ | $1.598\ 10^{-8}$ | 0.773 |
| 35 | $3.228\ 10^{-7}$ | $2.756\ 10^{-7}$ | 0.854 | $1.154\ 10^{-7}$ | $9.559\ 10^{-8}$ | 0.829 |
| 40 | $6.507\ 10^{-7}$ | $5.875\ 10^{-7}$ | 0.903 | $3.590\ 10^{-7}$ | $3.175\ 10^{-7}$ | 0.884 |
| 45 | $9.898\ 10^{-7}$ | $9.325\ 10^{-7}$ | 0.942 | $6.746\ 10^{-7}$ | $6.278\ 10^{-7}$ | 0.931 |
| 50 | $1.305\ 10^{-6}$ | $1.252\ 10^{-6}$ | 0.960 | $9.809\ 10^{-7}$ | $9.332\ 10^{-7}$ | 0.951 |

[a] Temperature independent cross-section. $J_{rel}$ relative values $J(T)/J(295\ K)$.

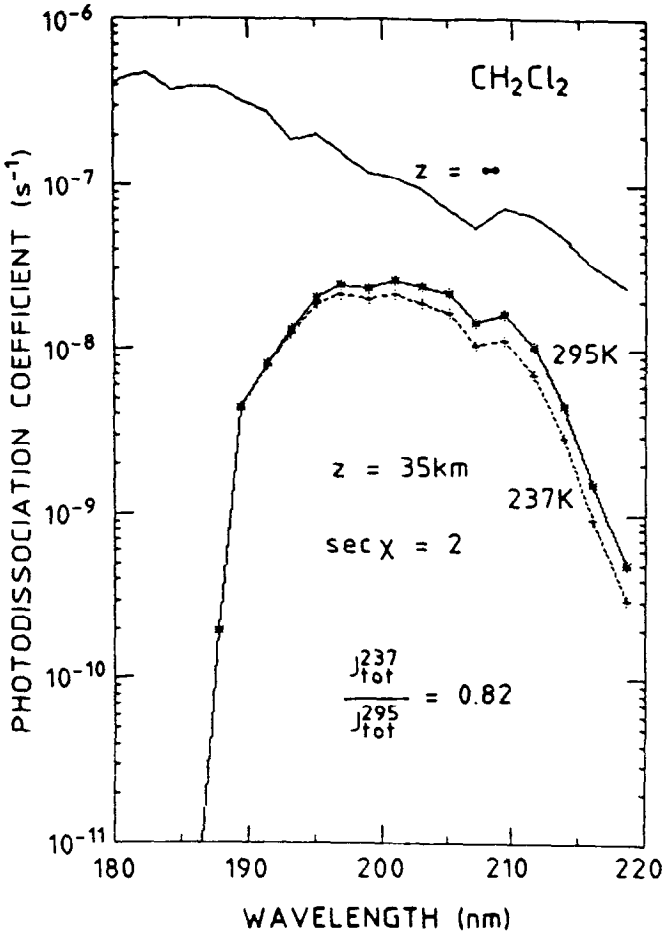


Fig. 10. Spectral distribution of photodissociation coefficients of $CH_2Cl_2$ for frequency intervals of 500 $cm^{-1}$, $z = 35$ km and solar zenith angle = 60° (sec $\chi = 2$). (*): $J(295\ K)$, (+): $J(237\ K)$.

Due to the significant increase of the ozone optical depth in the stratosphere at wavelengths beyond 220 nm, the value of the overall photodissociation coefficients between 20 and 35 km is mainly influenced by the 200–210 nm interval contribution.

In such conditions, a significant reduction of overall photodissociation coefficients is only to be expected in the case of compounds whose absorption cross-sections are strongly temperature-dependent in this wavelength interval. Accordingly, important reduction factors are observed for $CH_2Cl_2$, $CHCl_3$, $CF_2Cl_2$, and $CHFCl_2$ and, to a lesser extent for $CH_3Cl$, $CHF_2Cl$, and $CFCl_3$, while the $CCl_4$ photodissociation coefficient is almost temperature-independent in the stratosphere.

The introduction of lower photodissociation coefficients in atmospheric models increases altitudes of photolysis and, therefore, changes the altitude profile of the considered halomethane in the stratosphere.

In conclusion, this work presents a complete and coherent set of experimental data about temperature-dependent absorption cross-sections and photodissociation coefficients of chloro- and chlorofluoromethanes, and gives fairly simple relationships to compute the absorption cross-section values with respect to temperature and wavelength.

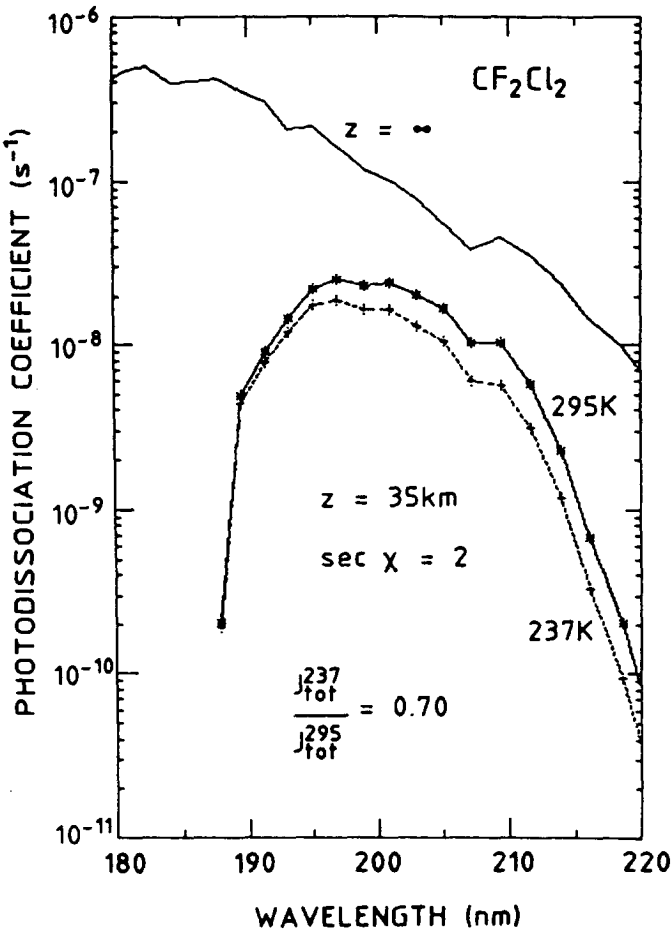


Fig. 11. Spectral distribution of photodissociation coefficients of $CF_2Cl_2$ for frequency intervals of 500 $cm^{-1}$, $z = 35$ km and solar zenith angle = 60° (sec $\chi = 2$). (*): $J$(295 K), (+): $J$(237 K).

## Acknowledgements

The authors wish to thank Dr G. Brasseur for helpful discussions and Mr E. Falise who performed the computer calculations of the photodissociation coefficients. This research has been partially supported by the European Community Commission under contract No. 303-78-1.

## References

Bass, A. M. and Ledford, A. E. Jr., 1976, Ultraviolet photoabsorption cross-sections of $CF_2Cl_2$ and $CFCl_3$ as a function of temperature, *12th Int. Conf. on Photochemistry, Gaithersburg (U.S.A.)*, June 1976.

Baulch, D. L., Cox, R. A., Crutzen, P. J., Hampson, Jr., R. F., Kerr, J. A., Troe, J., and Watson, R. T., 1982, Evaluated kinetics and photochemical data for atmospheric chemistry: supplement I, CODATA Task Group on Chemical Kinetics, *J. Phys. Chem. Ref. Data* **11**, 327–496.

Brasseur, G. and Simon, P. C., 1981, Stratospheric and thermal response to long-term variability in solar UV irradiance, *J. Geophys. Res.* **86**, 7343.

Chou, C. C., Vera Ruiz, H., Moe, K., and Rowland, F. S., 1976, Unpublished data, 1976, reported by Watson, R. T. (1977).

Chou, C. C., Smith, W. S., Vera Ruiz, H., Moe, K., Crescentini, G., Molina, M. J., and Rowland, F. S., 1977, The temperature dependences of the ultraviolet absorption cross-sections of $CCl_2F_2$ and $CCl_3F$, and their stratospheric significance, *J. Phys. Chem.* **81**, 286-290.

Chou, C. C., Milstein, R. J., Smith, W. S., Vera Ruiz, H., Molina, M. J., and Rowland, F. S., 1978, Stratospheric photodissociation of several saturated perhalo chlorofluorocarbon compounds in current technological use (Fluorocarbons 13, 113, 114, 115), *J. Phys. Chem.* **82**, 1–7.

Demore, W. B., Margitan, J. J., Molina, M. J., Watson, R. T., Golden, D. M., Hampson, R. F. Kurylo, M. J., Howard, C. J., and Ravishankara, A. R., 1985, Chemical kinetics and photochemical data for use in stratospheric modeling, JPL publication 85–37.

Fabian, P., Borchers, R., Penkett, S. A., and Prosser, N. J. D., 1981, Halocarbons in the stratosphere, *Nature* **294**, 733–735.

Gillotay, D. and Simon, P. C., 1988, Ultraviolet absorption cross-sections of methyl bromide at stratospheric temperatures, *Ann. Geophysicae* **6**, 211–215.

Gordus, A. A. and Bernstein, R. B., 1954, Isotope effect in continuous ultraviolet absorption spectra: Methyl bromide-$d_3$ and chloroform-*d*, *J. Chem. Phys.* **22**, 790.

Hubrich, C., and Zetzsch, C., and Stuhl, F., 1977, Absorptionsspektren von halogenierten Methanenen im Bereich von 275 bis 160 nm bei Temperaturen von 298 and 208 K, *Ber. Bunsenges. Physik. Chem.* **81**, 437–442.

Hubrich, C. and Stuhl, F., 1980, The ultraviolet absorption of some halogenated methanes and ethanes of atmospheric interest, *J. Photochem.* **12**, 93–107.

Kockarts, G., 1976, Absorption and photodissociation in the Schumann–Runge bands of molecular oxygen in the terrestrial atmosphere, *Planet. Space Sci.* **24**, 589–604.

Majer, J. R. and Simons, J. P., 1964, Photochemical processes in halogenated compounds, in J. Pitts, G. Hammond, and W. A. Noyes (eds.), *Advances in Photochemistry* vol. 2, p. 137.

Nicolet, M., 1984, On the molecular scattering in the terrestrial atmosphere: an empirical formula for calculation in the homosphere, *Planet. Space Sci.* **32**, 1467–1468.

Molina, M. J. and Rowland, F. S., 1974, Stratospheric sink for chlorofluoromethanes: chlorine atom-catalysed destruction of ozone, *Nature* **249**, 810–812.

Rebbert, R. E. and Ausloos, P. J., 1976, Gas-phase photodecomposition of carbon tetrachloride, *J. Photochem.* **6**, 265–276.

Robbins, D. E., 1976, Photodissociation of methyl chloride and methyl bromide in atmosphere, *Geophys. Res. Lett.* **3**, 213–216.

Robbins, D. E., 1976, Erratum, *Geophys. Res. Lett.* **3**, 757.

Robbins, D. E., 1976, UV photoabsorption cross sections for halocarbons, *Int. Conf. on the Stratosphere and Related Problems, Logan, (U.S.A.).*

Robbins, D. E. and Stolarski, R. S., 1976, Comparison of stratospheric ozone destruction by fluorocarbons 11, 12, 21, and 22, *Geophys. Res. Lett.* **3**, 603–606.

Rowland, F. S. and Molina, M. J., 1975, Chlorofluoromethanes in the environment, *Rev. Geophys. Space Phys.* **13**, 1.

Sandorfy, C., 1976, Review paper: UV absorption of halocarbons, *Atmos. Environ.* **10**, 343–351.

Schmidt, U., Knapska, D., and Penkett, S. A., 1985, A study of the vertical distribution of methyl chloride ($CH_3Cl$) in the midlatitude stratosphere, *J. Atmos. Chem.* **3**, 363–376.

Singh, H. B., Salas, L. J., Shigeishi, H., and Scribner, E., 1979, Atmospheric halocarbon, hydrocarbons, and sulfur hexafluoride: Global distribution, sources and sinks, *Science* **203**, 899–903.

Vanlaethem-Meuree, N., Wisemberg, J., and Simon, P. C., 1978, Influence de la température sur les sections efficaces d'absorption des chlorofluorométhanes dans l'ultraviolet, *Bull. Acad. Roy. Belgique, Cl. Sci.* **64**, 42.

Watson, R. T., 1977, Rate constants for reactions of $ClO_x$ of atmospheric interest, *J. Phys. Chem. Ref. Data* **6**, 871–917.

Wisemberg, J. and Vanlaethem-Meuree, N., 1978, Mesures des sections efficaces d'absorption de constituants atmosphériques dans l'ultra violet: description du système expérimental, *Bull. Acad. Roy. Belgique, Cl. Sci.* **64**, 21.

WMO, 1985, Atmospheric ozone 1985, WMO global ozone research and monitoring project, Report 16.

Wuebbles, D. J., 1983, Chlorocarbon emission scenarios: potential impact on stratospheric ozone, *J. Geophys. Res.* **88**, 1433–1443.